Speciation of Reactive Sulfur Species and their Reactions with Alkylating Agents: Do we have any clue about what is present inside the cell?

Virág Bogdándi,[1#] Tomoaki Ida,[2#] Thomas R. Sutton,[3#] Christopher Bianco,[4#] Tamás Ditrói,[1#] Grielof Koster,[3] Hillary A. Henthorn,[5] Magda Minnion,[3] John P. Toscano,[4] Albert van der Vliet,[6] Michael D. Pluth,[5] Martin Feelisch,[3] Jon M. Fukuto,[7] Takaaki Akaike[2*] and Péter Nagy[1*]

[1]*Department of Molecular Immunology and Toxicology, National Institute of Oncology, Ráth György utca 7-9, Budapest, Hungary, 1122*

[2]*Department of Environmental Medicine and Molecular Toxicology, Tohoku University Graduate School of Medicine, Sendai 980-8575, Japan.*

[3]*Clinical and Experimental Sciences, Faculty of Medicine, and University Hospital Southampton NHS Foundation Trust, University of Southampton, Southampton SO16 6YD, United Kingdom.*

[4] *Department of Chemistry, Johns Hopkins University, Baltimore, Maryland, 21218*

[5]*Department of Chemistry and Biochemistry, Materials Science Institute, Institute of Molecular Biology, University of Oregon, Eugene, OR 97403.*

[6]*Department of Pathology and Laboratory Medicine, Robert Larner M.D., College of Medicine, University of Vermont, USA.*

[7] *Department of Chemistry, Sonoma State University, Rohnert Park, CA 94928,*

Running Head: Speciation of Reactive Sulfur Species

[#] **These authors contributed equally to this study.**

***To whom correspondence may be addressed. E-mail:**

takaike@med.tohoku.ac.jp or peter.nagy@oncol.hu

This article has been accepted for publication and undergone full peer review but has not been through the copyediting, typesetting, pagination and proofreading process which may lead to differences between this version and the Version of Record. Please cite this article as doi: 10.1111/bph.14394

Abstract

Background and Purpose Posttranslational modifications of cysteine (Cys) residues represent a major aspect of redox biology, and their reliable detection is key in providing mechanistic insights. The metastable character of these modifications and cell lysis-induced artifactual oxidation render current state-of-the-art protocols to rely on alkylation-based stabilization of labile Cys derivatives before cell/tissue rupture. An untested assumption in these procedures is that for all Cys derivatives alkylation rates are faster than their dynamic interchange. However, when the interconversion of Cys derivatives is not rate-limiting, then electrophilic labeling is under Curtin-Hammett control and hence the final alkylated mixture may not represent the speciation that prevailed before alkylation.

Key Results We here present evidence that in the majority of cases, the speciation of alkylated polysulfide/thiol derivatives indeed depends on the experimental conditions. Our results reveal that alkylation perturbs sulfur speciation in both a concentration- and time-dependent manner, and that strong alkylating agents can cleave polysulfur chains. Moreover, we show that labeling of sulfenic acids with dimedone also affects Cys speciation, suggesting that part of the endogenous pool of products previously believed to represent sulfenic acid species may in fact represent polysulfides.

Experimental Approach These observations were obtained using buffered aqueous solutions of inorganic-, organic-, cysteine-, glutathione- and GAPDH-polysulfide species. Additional experiments in human plasma and serum revealed that monobromobimane can extract sulfide from the endogenous sulfur pool by shifting speciation equilibria, suggesting caution should be exercised when interpreting experimental results using this tool.

Conclusion and Implication We highlight methodological caveats potentially arising from these pitfalls and conclude that current derivatization strategies often fail to adequately capture physiologic speciation of sulfur species.

Keywords: cysteine oxidative posttranslational modifications, hydrogen sulfide, alkylation, polysulfides, sulfenic acid

List of abbreviations

3MST	3-Mercaptopyruvate sulfurtransferase
CBS	cystathione β-synthase
CSE	cystathione γ-lyase
DTNB	5-5'-dithiobis(2-nitrobenzoic acid)
DTT	dithiothreitol
HSA	human serum albumin
NADPH	Nicotinamide adenine dinucleotide phosphate
PVDF	polyvinylidene fluoride
ROS	reactive oxigen species
SDS PAGE	sodium dodecyl sulfate polyacrilamide gel electrophoresis
TCEP	Tris(2-carboxyethyl)phosphin
tRNA	transfer RNA
TTBS	tris-buffered saline and Tween 20 buffer
UV-vis	ultraviolet-visible
WT	wild type

Introduction

Hydrogen sulfide (H_2S) is now regarded as an important small bioactive molecule that orchestrates signaling events hand-in-hand with nitric oxide (Kevil *et al.*, 2017). A seminal paper by Mustafa and coworkers (Mustafa *et al.*, 2009), as well as subsequent work by others, provided evidence that persulfide (-SSH) and longer chain polysulfide ($-S_nH$) moieties on regulatory or functional protein Cys residues play a key role in transmitting sulfide-triggered biological events (Paul & Snyder, 2012; Ono *et al.*, 2014; Nagy, 2015). In addition, inorganic polysulfide species are thought to serve as important mediators in sulfide-based redox biology (e.g. (Nagy & Winterbourn, 2010a; Toohey, 2011; Greiner *et al.*, 2013; Cortese-Krott *et al.*, 2015; Kimura, 2017; Miyamoto *et al.*, 2017)). Although it is clear that sulfide/polysulfide-mediated cellular regulation is driven by redox chemistry, many mechanistic details remain elusive; this includes, for example, questions about the nature of the precursor molecule in a particular biological event and what drives the redox interconversion of sulfide/polysulfide/polythionate species. This uncertainty is partly due to the fact that, despite accumulating evidence underlying the importance of these reactive sulfur species (RSS) in biology, their reliable analysis still poses major challenges. On a more positive note, there has been a rapid evolution of sulfide and polysulfide detection protocols in the last few years, enabling a better understanding of the chemical biology of these species (Nagy *et al.*, 2014). For protein Cys polysulfide detection, the initially developed "switch techniques" (modified biotin switch assay (Mustafa *et al.*, 2009) and tag-switch techniques (Zhang *et al.*, 2014)) were followed by ProPerDP (Doka *et al.*, 2016; Doka *et al.*, 2017), which separates Cys thiols from Cys-polysulfides (after specifically pulling them down with biotinylated alkylating agents) by utilizing the reducibility of alkylated polysulfides as opposed to the non-reducible nature of alkylated thiols. This method was published along with conceptually similar techniques introduced by other groups (Gao *et al.*, 2015; Longen *et al.*, 2016). Furthermore, a recent protocol called polyethylene glycol-conjugated maleimide-labeling gel shift assay (PMSA) utilizes the cleavability of polysulfide chains by strong electrophiles and detection of protein polysulfide species based on mobility shifts on gels as a result of binding or cleavage of PEGylated alkylating agents (Akaike *et al.*, 2017).

Each of these techniques relies on initial electrophilic labeling of thiols and polysulfides with a particular alkylating agent, attempting to "freeze" their dynamic redox chemical reactions by generating relatively stable thioether or dialkyl polysulfide species. However, an understanding of the basic chemistry involved with these assays indicates that

caution must be exercised when interpreting data from experiments utilizing these reagents. Specifically, if sulfur species are in a dynamic redox equilibrium, then the levels of the various alkylated species will be a function of the relative rates of electrophilic trapping versus the redox equilibrium interconversions of the trappable species (which depend on a number of different parameters, e.g. concentrations, pH, and temperature). In essence, one would expect the electrophilic labeling of these polysulfides to be under Curtin-Hammett control (Seeman, 1986), meaning that due to fast interconversion between different polysulfides the mixture of alkyl polysulfides observed are a reflection of the relative rates of quenching rather than a representation of the true equilibrium. In other words, the observed labelled species may indicate the relative *reactivity* of the individual polysulfides rather than their actual *concentrations* (for a more detailed interpretation of this notion supported with chemical equations (reactions 1-7) please consult the Supporting Information). Hence, the initial electrophilic alkylation is a crucial step regarding the adequacy of the readouts of the particular method in light of the real speciation of the sulfur species to be detected. Similar problems were noticed in the early days of redox biology when methods were developed for Cys-thiol and disulfide species detection. For example, acidification was used initially to slow down redox events of thiol groups during cell lysis or tissue homogenization, although this is not necessarily sufficient to fully prevent artifactual redox reactions. This led to the use of cell permeable alkylating agents to avoid lysis-induced oxidation of reactive thiols. However, both the identity and concentration of the applied alkylating agent (e.g., *N*-ethylmaleimide (NEM), iodoacetamide (IAM) or S-methyl methanethiosulfonate (MMTS)) makes a difference in the detected oxidation state of protein thiol species, which was demonstrated for peroxiredoxins (Kumar *et al.*, 2013; Sobotta *et al.*, 2013). Despite these observations a large body of the redox biology literature tends to ignore these phenomena.

Here, we highlight important chemical aspects of alkylation steps from a mechanistic viewpoint, and experimentally demonstrate their impact particularly on the detection of polysulfides. Using inorganic polysulfides as well as cysteine, glutathione and protein-polysulfide systems, the speciation of polysulfide species of different chain lengths was investigated in a time and concentration resolved manner using different alkylating agents. Our investigations focused on two important chemical phenomena: 1) Speciation is likely to be under Curtin-Hammett control, so when alkylation is rate-determining, the equilibria that describe sulfur species speciation can be shifted during the alkylation process and confine the

measurements, and 2) certain alkylating alkylating agents have the ability to cleave polysulfur chains, even in already alkylated dialkyl polysulfide species.

Importantly, we obtained evidence that specific labeling of Cys sulfenic acids (Cys-OH) with dimedone can also affect Cys speciation. Specifically, we detected larger amounts of dimedone-labelled protein Cys upon treatment of GAPDH with inorganic polysulfides (which is not expected to directly induce Cys-OH formation) compared to when the protein was untreated or treated with H_2O_2 (which is known to induce Cys-OH formation).

Speciation in biological systems is further complicated by the interplay between inorganic and organic sulfur species and the compartmentalization of concurrent reactions.

Finally, using the state-of-the-art monobromobimane (MBB) derivatization based H_2S detection protocol in human serum and plasma we demonstrated that the amounts of sulfide detected largely depend on the applied concentration of MBB and the time of incubation with the alkylating agent. This observation is consistent with our previous proposal that speciation equilibria in biological sulfide pools are expected to be shifted towards sulfide production when sulfide is irreversibly derivatized during the detection protocol (Nagy *et al.*, 2014).

Materials and Methods

Materials

Most reagents, including anhydrous sodium sulfide (Na_2S) and sodium hydrosulfide (NaSH), were purchased from Sigma-Aldrich (Budapest, Hungary or Gillingham, UK), Nacalai Tesque (Kyoto, Japan), Wako Pure Chemical Industries (Osaka, Japan) or Invitrogen (Carlsbad, CA). Defined sodium polysulfide salts were provided by Dojindo Laboratories (Munich, Germany and Kumamoto, Japan). Tetrabutyl ammonium sulfide (NBu_4SH) was prepared as described in the literature (Hartle *et al.*, 2015). Sulfide stock solutions were prepared as previously described (Nagy *et al.*, 2014). Polysulfide stock solutions were prepared in either ultra-pure water or in the indicated buffer by dissolving either technical potassium polysulfide (K_2S_x; a mixture of polysulfides of different chain lengths), sodium disulfide (Na_2S_2), sodium trisulfide (Na_2S_3) or sodium tetrasulfide (Na_2S_4) salts. All solutions were prepared fresh immediately before use in experiments.

Speciation of inorganic polysulfides (Figs 1-3, Table 1 and Figs S1-S4)

Direct infusion experiments

Polysulfide solutions were prepared in either ultra-pure water or pH 7.4 ammonium phosphate buffer from different starting salts, mixed potassium polysulfide (K_2S_x), sodium disulfide (Na_2S_2), sodium trisulfide (Na_2S_3) and sodium tetrasulfide (Na_2S_4) to an approximate concentration of 10 mM and diluted 100-fold before being infused into the ESI source of the mass spectrometer for recording of the resulting mass spectra. IAM was then added to the remaining polysulfide solution from a 100 mM IAM stock (1% of polysulfide solution volume, resulting in a final concentration of 1 mM IAM) and allowed to react for at least 30 min before analysis. Either solution was infused for 1 min at a flow rate of 8 µl/min and scanned at a rate of 1 scan per second in the presence of ammonium acetate to enhance ionisation efficiency. Underivatized polysulfide solutions were analysed in negative ionisation mode while derivatized polysulfide solutions were monitored in both negative and positive ionisation mode. Negative ionisation mode was used to confirm the absence of unreacted polysulfides and positive mode was used to monitor the presence of alkylated polysulfide species. High-resolution mass spectra were recorded using a Waters SYNAPT G2-Si ESI-ToF-MS (time of flight mass spectrometer) calibrated using sodium formate clusters, and using standard conditions in the same manner as for the triple quadrupole analysis.

UHPLC-MS/MS set-up

Polysulfide solutions were prepared as before by addition of pre-weighed dry powder standards to ultra-pure water using either K_2S_x, Na_2S_2, Na_2S_3 or Na_2S_4. The polysulfide solution was then diluted 100-fold in different concentrations of either NEM or IAM (0.5, 1.0, 2.0, 5.0, 9.9, 39.6, 79.2 and 99.0 mM) in pH 7.4 ammonium phosphate buffer. In a separate set of experiments aimed at providing insight into the speed and pH sensitivity of polysulfide equilibration before derivatization, NEM and IAM alkylation reactions of polysulfide solutions were compared side-by-side using three different iterations: 1. Direct addition of accurately weighed dry polysulfide material to an appropriate volume of NEM or IAM-containing buffer pH 7.4; 2. Dissolution of dry polysulfides in ultrapure water (yielding an alkaline stock solution), dilution in buffer pH 7.4, followed by derivatization; and 3. Dissolution of dry polysulfides in buffer pH 7.4, followed by derivatization after a defined period of equilibration (see Supplementary Information for details).

To test the potential ability of NEM to attack the middle of, or break up polysulfide chains 1.9 mg Na_2S_4 was added to 10 mL IAM in ammonium phosphate buffer (10 mM IAM, final concentration Na_2S_4 1.09 mM) and allowed to react at room temperature for 10 min. An extension of the incubation time for IAM alkylation to 60 min did not change the outcome of the results. 100 µL of this solution was then added to 900 µL of 10 mM NEM and left at room temperature for a further 10 min and analyzed.

The polysulfide composition was analysed by UHPLC-MS/MS using a Waters Aquity UPLC system coupled with a Xevo TQ-S detector. Mobile phase A consisted of H_2O with 5 mM ammonium acetate; mobile phase B was 95% acetonitrile, 5% H_2O with 5 mM ammonium acetate. An Aquity UPLC CSH C18 (1.7 µm), 2.1 x 100 mm column was used for the separation using a chromatographic gradient starting at 95% A and decreased to 40% A over 5 min, the gradient then returned to 95% A over 1 min and was held for a further min to equilibrate the column. The flow rate was 0.2 ml/min, column temperature 30 °C and the injection volume used was 5 µL. Alkylated polysulfide species were detected using multiple reaction monitoring (MRM) mode using the precursor and product ion pairs described in the Supplementary Information. For the NEM-derivatized species a cone energy of 8 V and a collision energy of 14 V was used. For the IAM-derivatized species the cone energy was 8 V and collision energy was 12 V.

Alternate chromatographic separation for validation purposes (Figs 3E&F, S2, S3 and Scheme S1) was performed using the same chromatographic system and utilizing the same mass spectrometry detection. Mobile phase A consisted of H_2O with 5 mM ammonium formate and 0.15% formic acid, mobile phase B consisted of 95% acetonitrile, 5% H_2O with 5 mM ammonium formate and 0.15% formic acid. A 1.6 µm Modus 100 x 2.1 mm Aqua mixed mode UHPLC column was used for the separation using a chromatographic gradient starting at 99% A, decreasing to 60% A over 4.5 min, the gradient was then decreased to 0% A over 0.5 min and held for 1.5 min before increasing back to 99% A over 0.5 min and being held at 99% A for a further 1.0 min to equilibrate the column. The flow rate was 0.2 mL/min, column temperature 30 ^{o}C and the injection volume 5 µL. For MRM parameters see Table S1A.

Quantitative HPLC/MS-MS analysis of alkylated cysteine and glutathione polysulfur species (Figs 4-5 and S5-S8)

ß-(4-Hydroxyphenyl)ethyl iodoacetamide (HPE-IAM), MBB and NEM stock solutions (1 M) were prepared by dissolving the appropriate amount of solid chemicals in DMSO with further dilution in the indicated aqueous media. Polysulfidated Cys or GSH species were prepared by mixing 100 µM Cys or GSH with 300 µM Na_2S_2 in 30 mM HEPES/KOH buffer (pH 7.5) at room temperature for 5 minutes. Then, samples were incubated with 0.1-10 mM alkylating agent (0.1, 0.5, 1, 5 and 10 mM HPE–IAM, MBB or NEM respectively) at room temperature for 30 minutes, 60 minutes, 3 hours or 6 hours. After alkylation, samples were diluted with 0.1% formic acid (25-fold dilution) and LC-ESI-MS/MS analysis was performed on a triple quadrupole (Q) mass spectrometer LCMS-8050 (Shimadzu) coupled to the Nexera UHPLC system (Shimadzu) after addition of the appropriate internal standards. Per/polysulfide derivatives were separated by a Nexera UHPLC with a YMC-Triart C18 column (50 × 2.0 mm inner diameter) under the following elution conditions: mobile phases A (0.1% formic acid) with a linear gradient of mobile phases B (0.1% formic acid in methanol) from 5 to 90% for 15 min at a flow rate of 0.2 mL/min at 40 °C. The temperatures of the ESI probe, desolvation line, and heat block were 300, 250, and 400 °C, respectively; and the nebulizer, heating, and drying nitrogen gas flows were set to 3, 10, and 10 L/min, respectively. Various per/polysulfide derivatives were identified and quantified by means of multiple reaction monitoring (MRM) according to our previous report (Akaike *et al.*, 2017). MRM parameters of various per/polysulfide derivatives used for LC-MS/MS analyses are shown in Supplementary Table 1. Three different samples were prepared on three independent days for each condition.

Detection of sulfide in human serum or plasma (Fig 6)

Peripheral venous blood was collected from the antecubital vein of healthy human adults following informed consent using a procedure approved by the Hungarian National Ethics Committee (file number BPR-021/00084-2/2014). Blood samples were collected into serum or EDTA collection tubes. EDTA blood was immediately centrifuged at 3000 rpm for 10 min

and serum was obtained after centrifugation of blood that was allowed to clot at room temperature for 30 min. The supernatant serum or plasma samples were aliquoted into equal volumes and stored at -80 °C until use.

To follow the kinetics of sulfide-dibimane formation (the product of MBB-derivatized sulfide, which is measured during the monobromobimane method for sulfide detection (Nagy *et al.*, 2014)) in blood samples or standard sulfide solutions, 250 µL of plasma, serum or 100 µM H_2S stock solution was mixed with 650 µL of 200 mM HEPES buffer, pH 8.2 and 10 µL of 100 mM MBB in acetonitrile. The derivatization reaction proceeded in the dark at room temperature. After defined time periods 70 µL aliquots from the reaction mixtures were withdrawn and mixed vigorously with 5 µL 50% trichloroacetic acid to stop the alkylation process. Samples were centrifuged (30,000 g/5 min) and the supernatants stored in the autosampler in dark vials at 5 °C.

A Thermo Ultimate 3000 HLPC system equipped with fluorescent detector was used with a Zorbax Eclipse XDB-C18 column (250x4.6 mm, 5 µm, Agilent) for the separation of the analytes. 10 µL of the derivatized sample was injected and eluted using a 35 minute long gradient profile consisting of 0.1% of formic acid (A) and 0.1% of formic acid in acetonitrile (B) at a 1mL/min flow rate. The gradient profile started with 15% B and increased to 30% in 3 minutes. After 8 minutes of isocratic elution, the composition increased to 90% B in 2 minutes and stayed there for another minute before returning to the initial 5% B. The fluorescence detector was set to 390 nm (excitation wavelength) and 475 nm (emission wavelength) to detect and quantitate the product sulfide-dibimane. Sulfide concentrations were calculated based on calibration curves established using derivatized standard sulfide solutions in water together with calibration blanks (deionized water). Standards (1-5 µM) were prepared by serial dilution of a 50 µM derivatized stock using deionized water.

Biotin-polyethylene glycol (PEG)-conjugated maleimide (biotin-PEG-MAL) labeling gel shift assay (PMSA) for GAPDH (Fig 7)

The assay was performed as reported previously with slight modifications (Jung *et al.*, 2016; Akaike *et al.*, 2017). Briefly, purified recombinant human GAPDH (stored at –80 °C) was applied to a PD SpinTrap G-25 column (GE Healthcare, Little Chalfont, England) previously equilibrated with RIPA buffer (10 mM Tris-HCl, 1% NP-40, 0.1% sodium deoxycholate,

0.1% SDS, 150 mM NaCl, pH 7.4) to remove reductants. Desalted protein samples were incubated with 1 mM or 10 mM Na_2S_2 or Na_2S_3 at 37 °C for 1 h. After incubation, excess inorganic polysulfides were removed by a second desalting step (same conditions as the first). Protein quantification was performed by the bicinchoninic acid assay to normalize the total protein content of each sample. Sulfhydryl groups were labelled by incubation with 2 mM biotin-PEG 36-maleimide (Dojindo Laboratories) reagent in RIPA buffer at 37 °C for 1 h. The labeled protein samples were subsequently incubated with various electrophile agents (IAM, MBB, NEM and DTNB, 3 mM each) at 37 °C for 1 h. Samples were stored at –20 °C after heating them to 95 ^{o}C for 5 min in the presence or absence of 5% 2-ME. Next day, SDS-PAGE and CBB staining were performed to assess the ability of the electrophiles (added after the biotin-PEG 36-maleimide labeling) to cleave dialkyl polysulfur chains as reported previously (Jung *et al.*, 2016; Akaike *et al.*, 2017).

Dimedone labeling of GAPDH-$(S)_n$-OH species (Fig 8)

GAPDH was incubated with 5 mM DTT at 4 °C for 30 minutes, and then desalted with a Zeba desalting spin column. Protein was quantified by the Bradford assay, before and after the prereduction step. 50 mM dimedone was added to the protein samples at room temperature. Within 1 min, samples were treated with 200 µM of H_2O_2 or Na_2S_2 or equal volume of buffer and incubated at room temperature for 60 min. Samples were digested with 14.4 mg/mL pronase at 37 °C for 60 min, then 50% TCA was added, followed by vortexing and centrifuging at 3000 g for 5 min. Supernatants were collected and LC/MS-MS analysis was performed on a Thermo LTQ-XL linear ion-trap mass spectrometer coupled to the Thermo Ultimate 3000 HPLC system. 50 µL of the samples were injected onto a Kinetex C18 column (50x2.1 mm, 2.6 µm, Phenomenex) and eluted using 0.1% formic acid in water (A) and 0.1% formic acid in methanol (B). The gradient started with 5% B linearly increasing to 95% in 15 minutes. Dimedone products were identified in positive ionization mode and quantified by single ion monitoring.

For the prealkylated experiments, after prereduction with DTT and desalting, samples were treated with 200 µM of H_2O_2 or Na_2S_2 at room temperature for 2 min, then incubated with 20 mM HPE-IAM at room temperature for 20 min. HPE-IAM excess was removed by desalting with a Zeba desalting spincolumn, then samples were incubated with 50 mM

dimedone at room temperature for 60 min. Pronase digestion and LC/MS-MS analysis was performed as previously mentioned. All treatments were carried out at pH 7.40, and dilutions were performed in 100 mM phosphate buffer containing 100 µM DTPA.

Equilibrium Analyses and Competitive Trapping of glutathione-polysulfur species (Fig 9)

NMR analyses

NMR analyses were performed using an Agilent 400 MHz NMR spectrometer. Water suppression for all samples was achieved using an (^{1}H) Presat method of vnmrj software. All NMR solvents were 10% D_2O in phosphate buffer (100 mM, pH 7.4) containing 1 mM 4,4-dimethyl-4-silapentane-1-sulfonic acid (DSS) as an internal standard. Stock solutions of GSSG (100 mM) and NaSH (50 and 100 mM) were prepared in phosphate buffer (100 mM, pH 7.4). DSS (internal standard) stock solutions (10 mM) were prepared in D_2O.

To investigate the NaSH/GSSG equilibrium 10 mM GSSG was mixed with 5, 10 or 15 mM NaSH in the NMR tube. Measurements were performed after 30 min equilibration at room temperature.

Competitive trapping of persulfides were achieved by incubating 5 mM NaSH with 10 mM GSSG in phosphate buffer (100 mM, pH 7.4) containing 1 mM DSS in an NMR tube. Reaction mixtures were equilibrated for 30 minutes at room temperature. IAM or NEM (0.5, 1, 1.5, 2 or 2.5 mM) was then added and reactions were allowed to proceed at room temperature for 1 hour, followed by ^{1}H NMR analyses.

Mass spectrometry analyses

Mass spectra were recorded using a Thermo Triple Quadrupole Electrospray Ionization Mass Spectrometer (ESI-MS) operating in positive ion mode and controlled with XCalibur 2.1 software. Samples were directly injected via syringe pump at a flow rate of 5 µl/min using N_2 as a sheath gas and Ar as a collision gas. Ion optics were optimized using authentic samples of disulfides. The capillary temperature was 250 °C and spray voltage was 2500 V. Stock solutions of GSSG (100 mM) and NaSH (50 mM) were prepared in ammonium bicarbonate buffer (50 mM, pH 7.4).

The NaSH/RSSR equilibrium was investigated by mixing 1 mM GSSG with 0.5 mM NaSH in ammonium bicarbonate buffer (50 mM, pH 7.4), and solutions were incubated at room temperature for 30 minutes before ESI-MS analysis.

The competitive trapping of persulfides was achieved by adding the indicated amounts of IAM or NEM to the above reaction mixture and then allowing the reactions to proceed for 1 more hour at room temperature, followed by ESI-MS analysis.

Inorganic polysulfide speciation in non–aqueous systems (*Fig 10 and Table 2*)

UV–Vis measurements

UV–Vis measurements were performed on a Cary 100 spectrophotometer equipped with a Quantum Northwest cuvette temperature controller under anaerobic conditions. 20 mM stock solution of S_8 was prepared in dry, air-free, deuterated tetrahydrofuran; stock solutions of NBu_4SH (20, 40, 60, 80, 160 mM) were made in dry air-free deuterated acetonitrile. Inorganic polysulfide solutions were prepared by mixing 0.5 mL of S_8 stock solution with 0.5 mL of the NBu_4SH solutions. The mixture was charged in either a septum-sealed short path quartz cuvette or into a small GC vial. Gas-tight Hamilton syringes were used for all solution transfers. Cuvettes were heated at 60° C until the UV-Vis spectra equilibrated; this was required to fully solvate the polysulfide mixture. Then, spectra were collected at 40° C and 25° C after a 15 minute equilibration period. Cuvettes were shaken before collecting spectra.

^1H NMR measurements

NMR spectra were acquired on a Bruker Avance-III-HD 600 spectrometer with a Prodigy multinuclear broadband CryoProbe. Polysulfide solutions in sealed GC vials were heated in a 60 °C sand bath while stirring for 1 hour. After 1 hour, the sand bath temperature was either not changed, or set to 40 °C or 25 °C. Once target temperatures were reached, the polysulfides were electrophilically trapped by the addition of triethylamine (6 equivalents) and benzyl chloride (6 equivalents). Dry DCM (1.3 μL) was added as a standard. The reaction mixtures were analyzed in an oven dried NMR tube sealed with septa caps.

Attempt to trap sulfur-centered radical species upon potential homolytic cleavage of polysulfide species using DMPO

To trap sulfur-centered radicals generated by the homolytic cleavage of the sulfur-sulfur bonds in per- and polysulfides, 5,5-Dimethyl-1-pyrroline-*N*-oxide (DMPO) was used as a trapping agent.

To investigate whether alkylated polysulfide species can undergo homolytic -S-S- bond cleavage we used alkylated glutathione (GSH) per- and polysulfides, which were prepared by mixing 20 mM GSH with 60 mM Na_2S_2 in 200 mM HEPES/HCl pH 7.5 for 5 min at room temperature. Next, the samples were alkylated with 40 mM IAM for 15 min at RT before the addition of 20 mM DMPO. The mixtures were placed in autosampler vials at 5 °C and 50 µL sample aliquots were injected every 40 min for 4 hours.

The measurements were carried out on a Thermo Ultimate 3000 HLPC system with a Kinetex C18 column (50x2.1 mm, 2.6 µm, Phenomenex) connected to a Thermo LTQ-XL linear ion-trap mass spectrometer. The samples were eluted using 0.1% formic acid in water (A) and 0.1% formic acid in methanol (B). The gradient started with 5% B linearly increasing to 95% in 15 minutes. DMPO adducts were monitored in positive ionization mode. The monitored parent m/z values were the following: 421 and 419 for GS-DMPO as hydroxylamine and nitrone adducts respectively and 114 for DMPO.

To investigate whether non-alkylated polysulfide species can undergo homolytic –S-S- bond cleavage we used (GSH) per- and polysulfide species, which were prepared by treating 1 mM glutathione with 1 mM Na_2S_2 in 200mM HEPES/HCl pH 7.5 for 5 min at RT. Next, 50 mM DMPO was added to the solution. Samples were injected directly into the mass spectrometer and detection of DMPO adduct formation was attempted in positive ionization mode.

Data analyses

Data analysis for the experiments described in Section Figures 3 and S3 were performed using Microsoft Excel and GraphPad Prism (GraphPard Software Inc.). For the experiments in Section Figures 4, 5 and S5-S8, data analysis was carried out using Microsoft Excel, plotted values show the averages and the corresponding error bars represent their standard

deviation. Data for the experiments in Figures 6 and 8 were fitted or evaluated using GraphPad Prism. Values on Figure 8 represent the average of data points, while the error bars show their standard error of mean. Data on Fig 9F show the average of three experiments and the error bars represent their standard deviation at each data point.

Results and Discussion

Speciation of inorganic polysulfide species

Inorganic polysulfide species have been suggested to be important mediators in biology (Greiner *et al.*, 2013; Kimura, 2017). They can be generated during mitochondrial oxidative catabolism (Powell & Somero, 1986; Bouillaud & Blachier, 2011; Jackson *et al.*, 2012; Modis *et al.*, 2014; Szabo *et al.*, 2014; Mishanina *et al.*, 2015), by metalloprotein-catalyzed oxidation of sulfide (Palinkas *et al.*, 2015; Bostelaar *et al.*, 2016; Padovani *et al.*, 2016; Garai *et al.*, 2017; Olson *et al.*, 2017; Vitvitsky *et al.*, 2017), or by reaction of sulfide with nitric oxide (Cortese-Krott *et al.*, 2015). Although direct oxidation of sulfide by ROS is relatively slow in many cases (Carballal *et al.*, 2011), the neutrophilic oxidant, hypochlorous acid (HOCl), can oxidize sulfide with a nearly diffusion controlled rate to produce inorganic polysulfides, which could be a relevant route of polysulfide production under certain biological conditions (e.g. at sites of inflammation) (Nagy & Winterbourn, 2010a). On mechanistic grounds, sulfide oxidation reactions most likely proceed via a sulfenic acid intermediate species (S-OH, just as in the case of cysteine).

$$H_2S + \text{oxidant} \rightleftharpoons \text{HS-OH} + \text{H-red} \qquad (7)$$

However, HS-OH has not yet been experimentally characterized by any means in biologically relevant oxidation processes of sulfide, likely due to its high reactivity and short-lived nature, although a recent study claims to have trapped HSOH and other oxidized sulfur species upon sulfide oxidation (Kumar & Farmer, 2018). The applied trapping methodology with alkylating agents in this latter study raises similar issues that are the subject of the present paper (for example the trapped HSOH could have originated from hydrolysis of polysulfides, as proposed in reaction 17; see below). The resulting sulfenic acid is expected to react rapidly with another sulfide molecule to produce a disulfide species (in analogy to the reaction of Cys-OH with Cys as we reported earlier (Nagy & Ashby, 2007)), which can then

further react via disproportionation and/or conproportionation reactions to provide a mixture of longer-chain polysulfides (equations 8-12 for illustration; many more reactions are possible. Differently charged states of the reactant/product species were not included for the sake of simplicity.):

$$HS\text{-}OH + H_2S \rightleftharpoons HSSH + H_2O \quad (8)$$

$$2\,HSSH \rightleftharpoons HS_3H + H_2S \quad (9)$$

$$HSSH + HS_3H \rightleftharpoons HS_4H + H_2S \quad (10)$$

$$HS_3H + HS_3H \rightleftharpoons HS_4H + HSSH \quad (11)$$

$$HS_3H + HS_3H \rightleftharpoons HS_5H + H_2S \quad (12)$$

Although the first report of inorganic polysulfides by Scheele dates back to 1777 (Scheele, 1777), and Berzelius crystallized the first polysulfide salt as early as 1822 (Berzelius, 1822), the solution inorganic chemistry of polysulfides is still not well understood. For example, the number of sulfur atoms in the longest possible polysulfide chain in aqueous media is still debated. Some say that it should be below 5 (Maronny, 1959; Giggenbach, 1972; Licht *et al.*, 1986; Licht, 1987), others argue that HS_6^- also has measurable stability (Cloke, 1963; Boulegue & Michard, 1978). Based on mass spectrometry measurements, Gun et al (Gun *et al.*, 2004) recently proposed that the number of sulfurs can reach even up to 9 in inorganic polysulfide chains. One reason for these controversial reports could be that interconversion of polysulfides can rapidly occur. The fact that a number of different polysulfides are typically present in solution at any given condition makes characterization of these species by UV, IR or Raman spectroscopy and chromatographic separation challenging. Hence, most studies that measure polysulfide speciation in solution use a derivatization step before separation and detection. However, mass spectrometry can in principle distinguish between polysulfides of different chain length even in the absence of chromatographic separation. Therefore, we used ESI-based mass spectrometry (for conditions see Materials and Methods) to investigate speciation in polysulfide solutions without derivatization by direct infusion of the solutions into the source. Due to their low pK_a ((Steudel, 2003a; Steudel, 2003b; Nagy, 2015), and hence good ionizability) polysulfides were detected in negative ionization mode during these experiments. We found that the dissolution of sodium trisulfide, tetrasulfide and mixed

potassium polysulfide salts in ultra-pure water all result in similar speciation patterns (Figure 1A-C).

Consistent with our previous investigations (Cortese-Krott *et al.*, 2015), the m/z of the most abundant species observed was the trisulfide radical anion ($S_3^{\bullet-}$). In addition, the peaks at m/z of ~64 and 128 were indicative of disulfide and tetrasulfide radical ion species ($S_2^{\bullet-}$ and $S_4^{\bullet-}$) formation. In order to confirm the tentative assignment of these polysulfide species as radical anions we used high-resolution mass spectrometry. The resolution of the ToF-MS used was sufficient to distinguish the additional mass of the electron (0.00054 amu) in a radical ion. Figure 1D shows the full mass spectrum (m/z 50-150) of a similar polysulfide solution as Figure 1A-C, recorded using the high-resolution SYNAPT G2-Si ESI-ToF-MS.

The peaks for the three polysulfide radical anions observed in the triple quadrupole experiments were detected at m/z 63.9469 for $S_2^{\bullet-}$, 95.9170 for $S_3^{\bullet-}$ and 127.9057 for $S_4^{\bullet-}$. There was also a mass peak detected for a thiosulfate radical anion at m/z 111.9312 and the protonated thiosulfate anion at m/z 112.9398. The peak at m/z 96.9599 corresponds closely to HSO_4^- (see Table 1 for details) whilst the peak with m/z = 128.9178 does not appear to be related to any protonated polysulfide anion (based on the exact mass and the isotope distribution pattern).

The exact calculated masses for the three polysulfide radical ions are as follows; $S_2^{\bullet-}$ m/z 63.9448, $S_3^{\bullet-}$ m/z 95.9168 and $S_4^{\bullet-}$ m/z 127.8890. The closest in mass among the detected peaks is the $S_3^{\bullet-}$ with a mass difference of only 0.0002 amu. The larger deviations from the theoretical masses of $S_2^{\bullet-}$ and $S_4^{\bullet-}$ (Table 1) may be due to the lower abundances of these two species; moreover, the mass of $S_2^{\bullet-}$ is close to the lower range of the ToF-MS (m/z 50) and detection compounded by the associated loss of resolution at that range.

To confirm that the measured m/z indeed represent radical anions as opposed to doubly charged anions with twice the number of sulfurs we investigated the isotope distribution patterns of these species. Due to the difference in atomic mass between ^{34}S and ^{32}S (1.9958 amu) and the low natural abundance of ^{33}S (0.75%) this can be used as an indicator of the charge states of the detected species since doubly charged species would show isotope peaks at M+1 and singly charged species at M+2. Figure 1E shows an expanded section of the spectrum showing the suggested $S_3^{\bullet-}$ peak and its +2 isotope peak at m/z 97.9128. If the peak at m/z 95.9168 was representative of a doubly charged anion (S_6^{2-}) there

would be a +1 isotope peak present with an intensity of ~12% of the parent peak. However, the spectra does not show a +1 isotope peak, but instead shows a +2 isotope peak at m/z 97.9128 with an exact difference of 1.9958 amu from the parent peak. Likewise, Figure 1F shows the same for $S_4^{\bullet-}$, again with no +1 isotope peak present but a corresponding + 2 isotope peak at m/z 127.9001 with a mass difference of 1.9944 amu from the parent peak. This isotope distribution pattern rules out the possibility of the observed m/z originating from doubly charged polysulfide anions. No isotope peak was observed for $S_2^{\bullet-}$, likely due to its low signal intensity. There were also no M+4 isotope peaks observed, which is not unexpected as the abundance of these species would be low enough to fall into the noise in the spectrum.

The high-resolution mass spectrometry experiments strengthen the previous assignment of the aqueous polysulfide species as radical anions. However, as a point of caution we note that the SYNAPT G2-Si ESI-ToF-MS uses the same ESI source as the TQD mass spectrometer used in the previous experiments. Therefore, if the polysulfide radical ions originated in the source or were due to the mechanism of ionization then no differences in the apparent speciation would be expected between these two experiments. Of note, we observed no major changes in speciation upon changing some mass spectrometry parameters (source temperature, voltage, flow rate). In agreement with this experimental experience, Gun *et al* also found that the source voltage and temperature had no observable effect on speciation of polysulfide species (Gun *et al.*, 2004). However, at their applied conditions they detected primarily longer-chain polysulfides and did not report the presence of any radical species. Their argument for the preferential detection of longer-chain polysulfides was that the charge of the detected ions is more evenly distributed on longer-chain polysulfides, which makes them more stable. They also argue that the distribution of the detected species is affected to a larger extent by their gas phase distribution, rather than solution stability. However, they used very long incubation times (12h) to equilibrate polysulfide speciation. Our own experience with polysulfide solutions indicate that most of the open-chain polysulfide species are much less stable at pH 7.4 and would not survive these long incubation times. Polysulfides with > 5 sulfurs have the ability to reside as homocyclic species, which have larger thermodynamic stabilities than their open-chain isomers under the applied conditions (Donohue, 1961). Therefore, we speculate that due to the long incubation times applied by Gun et al, it is conceivable that they mostly detected these more stable species whereas in our experiments

the open-chain polysulfides could undergo homolytic cleavage or $1e^-$ oxidation processes in the source of the mass spectrometers to yield polysulfide radical anion species.

Because of the labile nature of polysulfides, in most investigations these species are derivatized before separation and detection. Kamyshny's group published a series of rigorous investigations on the speciation and detection of inorganic polysulfides under different conditions (Donohue, 1961; Cotgreave & Moldeus, 1986; Kamyshny *et al.*, 2004; Kamyshny *et al.*, 2006; Kamyshny *et al.*, 2007; Kamyshny *et al.*, 2009). They realized that it is of utmost importance to make the derivatization step faster than the interconversion of polysulfide species to derive meaningful readouts. However, the large number of possible reactions that can affect polysulfide speciation pose serious challenges for studying the kinetics and mechanisms of these reactions. Despite these limitations, basic kinetic and isotope labelling studies demonstrated that by using methyl trifluoromethane-sulfonate (triflate) at adequate concentrations in simple aqueous buffer systems, some interconversion reactions could be ruled out to be faster than the actual derivatization steps (Kamyshny *et al.*, 2004). Unfortunately, the situation is much more complex in biological systems, and this phenomenon has not been studied with respect to the more commonly used cell-permeable alkylating agents such as NEM, IAM or MBB.

In order to assess whether alkylation impacts speciation, we first attempted to derivatize polysulfide species in buffered aqueous solution using a high concentration (100 mM) of the alkylating agent iodoacetamide. Figure 2A is recorded in positive ion mode to detect IAM alkylated polysulfide species, and Figure 2B shows the spectrum obtained with negative ionization of the same solution, confirming no residual underivatized polysulfide species remained. The most abundant derivatized species detected was the disulfide (IAM_2-S_2), followed by trisulfide (IAM_2-S_3), and the least abundant was the tetrasulfide (IAM_2-S_4). This speciation is not vastly different in terms of number of sulfurs in the polysulfide chain compared to those in Figure 1. Therefore, if the polysulfide radical anion species are generated via homolytic cleavages of longer polysulfide chains, then the derivatization has changed speciation substantially. We however believe that the presence of radical species in the source is likely to be largely due to in-source oxidation of polysulfides as a result of the ionization process.

Next, we examined how derivatization by NEM and IAM at different alkylating agent concentrations impacts polysulfide speciation using UHPLC separation and MS/MS detection. Under the applied conditions (see Materials and Methods section 1.2.2.), NEM-

derivatized polysulfides can be separated by our method with increasing number of sulfurs from S_1-S_4 eluting from 4.85 min to 6.45 min (Figure 3A); higher than S_4 NEM-derivatized polysulfides were not observed. IAM-derivatized polysulfides also separate well with increasing number of sulfurs from S_1-S_7 eluting in the range of 1.85 min to 4.80 min (Figure 3B). Regardless of whether the starting polysulfide solution was made up using a mixed potassium polysulfide or pure sodium tri- or tetrasulfide, the speciation pattern looked very similar, consistent with the direct infusion experiments displayed in Figure 1. However, the applied concentrations of NEM or IAM did have an impact on the apparent speciation of derivatized polysulfides.

Using NEM, the average length of detected polysulfide chains tended to decrease with increasing NEM concentrations (Figure 3C). With IAM alkylation the speciation under the conditions of Figure 3D seems to be stable and independent of IAM concentration. It should be noted that when we used lower concentrations of polysulfide solutions (10 μM) only S_1 and S_2 were detected across the whole concentration range for NEM and S_1 - S_3 for IAM (not shown). This is potentially due to the abundance of the larger polysulfides dropping below the limit of detection due to the lower overall sulfane sulfur concentration. The lack of signal for the longer polysulfides may also be due to slower disproportionation of the smaller polysulfides (being a second order process the half-life depends on overall concentration) to the potentially more stable longer-chain polysulfides compared to the rate of derivatization under these conditions (pseudo first-order process, where the half-life depends on alkylating agent concentration only).

To investigate further the suitability of IAM to detect speciation in simple inorganic polysulfide solutions, the effects of the exact composition and order of mixing of the starting solutions were investigated. This experiment confirmed that under four different experimental conditions no significant impact on the speciation of derivatized polysulfides was observed (Figure S1A). However, when using NEM as the derivatization agent, the starting conditions do appear to have an effect on polysulfide speciation (Figure S1B). This is likely due to the shift of polysulfide distribution equilibria during alkylation by NEM more so than by IAM under the applied conditions. This assumption was confirmed in additional experiments using alternative chromatography (Fig. S2) but identical MS detection conditions and NEM and IAM in direct comparison side-by-side. In incubations with NEM, the highest polysulfide species observed corresponded to the polysulfide salt used as starting material whilst with IAM also longer polysulfide chains were observed (see Fig. S3). This

observation could be interpreted such that faster alkylation reactions with NEM prevent formation of longer-chain polysulfides via disproportionation/conproportionation (see reactions 8-12) reactions, while slower alkylation with IAM does not. However, apparent speciation differed little regardless of whether defined polysulfide salts were directly dissolved as solids in the presence of an excess of alkylating agent or whether they were allowed to first equlibrate at alkaline or physiological pH before being derivatized (Fig. 3E, 3F and S3; see also Suppl. Scheme 1 for specific reaction conditions). This observation is consistent with faster equilibration of polysulfide speciation compared to the rates of the alkylation reactions.

Another important consideration in this context is the different mode of alkylation of polysulfides by NEM and IAM and the very different chemistries (and hence kinetics) involved: NEM is a strong electrophile with an activated double bond that reacts with nucleophiles such as thiols and polysulfides via a Michael addition reaction, while substitution of the iodine in IAM against the sulfane sulfur of a polysulfide chain is a nucleophilic substitution (S_N2) reaction:

Reaction 13: Alkylation with NEM (nucleophilic addition)

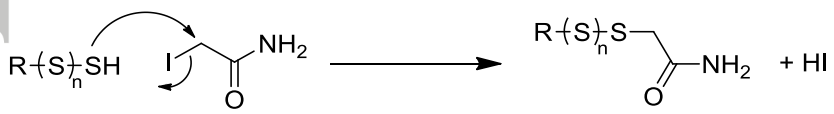

Reaction 14: Alkylation with IAM (nucleophilic substitution)

Importantly, these reactions have to proceed twice before both ends of the polysulfide chain are alkylated (and presumably protected from further equilibration). The chemical properties of the first reaction product (i.e. with inorganic polysulfides where R=H in reactions 13 and

14) are likely to be critical for fate and speed with which the second reaction can take place, but nothing is known about these details.

A recent study observed that, in contrast to IAM, NEM can cleave dialkyl polysulfide chains, thus making it unsuitable for longer-chain polysulfide species detection (Akaike *et al.*, 2017). To test if NEM is able to attack mid-chain sulfurs in inorganic polysulfides (as opposed to just reacting with the end-chain sulfurs), polysulfide solutions were first fully reacted with a 10-fold molar excess of IAM before addition of NEM; at this stage there should be no end-chain sulfurs left to react with, based on the data shown in Figure 2. After addition of NEM to the IAM-derivatized polysulfide solutions, IAM-derivatized S_1, S_2 and S_3 were still observed but in lower abundance than before NEM addition (Figure S4) and no longer-chain polysulfides were detected (which may also be due to the relative low concentration of sodium tetrasulfide used). Also observed after NEM addition were hybrid polysulfide adducts with one carboxamidomethyl moiety (from IAM) and one succinimide (from NEM) for S_1, S_2 and S_3. This suggests that NEM had reacted with the sulfide chain at non-terminal sulfurs, leading to a cleavage of the polysulfur chain. The mechanism of this reaction is unclear and somewhat unexpected as it further suggests that NEM can react with polysulfides by a mechanism other than nucleophilic addition. A few possible models to explain these observations are presented as follows:

Heterolytic cleavage: It is conceivable that what precedes reaction with NEM is a heterolytic S-S bond cleavage of the fully derivatized IAM-polysulfide adduct with formation of one carboxamidosulfur chain with a positive charge and another one with a negative charge; in a second step the negatively charged IAM-(poly)sulfide then reacts with NEM to form the hybrid polysulfide adduct (Reaction 15).

Homolytic cleavage: Alternatively, end-capped polysulfides (i.e. $(IAM)_2S_x$ compounds) may have a tendency to cleave homolytically and the IAM-S_x radical species formed then adds to the double bond of NEM (Reaction 16). Similar reactions may occur with the corresponding NEM-polysulfide adducts. Such a behaviour would also be consistent with another recent observation, i.e. that the NEM adduct of S_2^{2-} is not stable at pH 7.4 (Sutton *et al.*, 2018), supporting the notion that NEM- and IAM-derivatized polysulfide adducts are metastable and both, NEM-S and IAM-S are good leaving groups. We used DMPO trying to capture sulfur-centered products generated upon homolytic cleavage of glutathione polysulfide species

under two different conditions (using alkylated polysulfides and non-alkylated polysulfides), but were unable to detect DMPO adducts under any experimental condition (see Methods).

Hydrolysis: Mechanistically, electrophilic addition-based alkylation by NEM could also shift the hydrolysis of longer-chain polysulfide equilibria (as shown below) to the right (which would be expected to shift to the left in the absence of NEM) and eventually generate shorter-chain alkylated species and the corresponding alkylated sulfenic acid (Reaction 17). This model would predict that specific sulfenic acid capturing tools such as dimedone might also shift reaction 17 to the right. If true, this could result in eventual dimedone capturing of Cys residues that were originally present as polysulfides. This is in fact a plausible caveat of sulfenylation measurement protocols, which we specifically address in experimental models using GAPDH, see below.

Direct reaction between the alkylating agents and sulfurs within the polysulfide chain: Alkylating agents could also attack a mid-chain sulfur bond. The reactivity of IAM and NEM is expected to be largely different in these reactions due to the fundamentally different chemistries involved (Models 18 and 19).

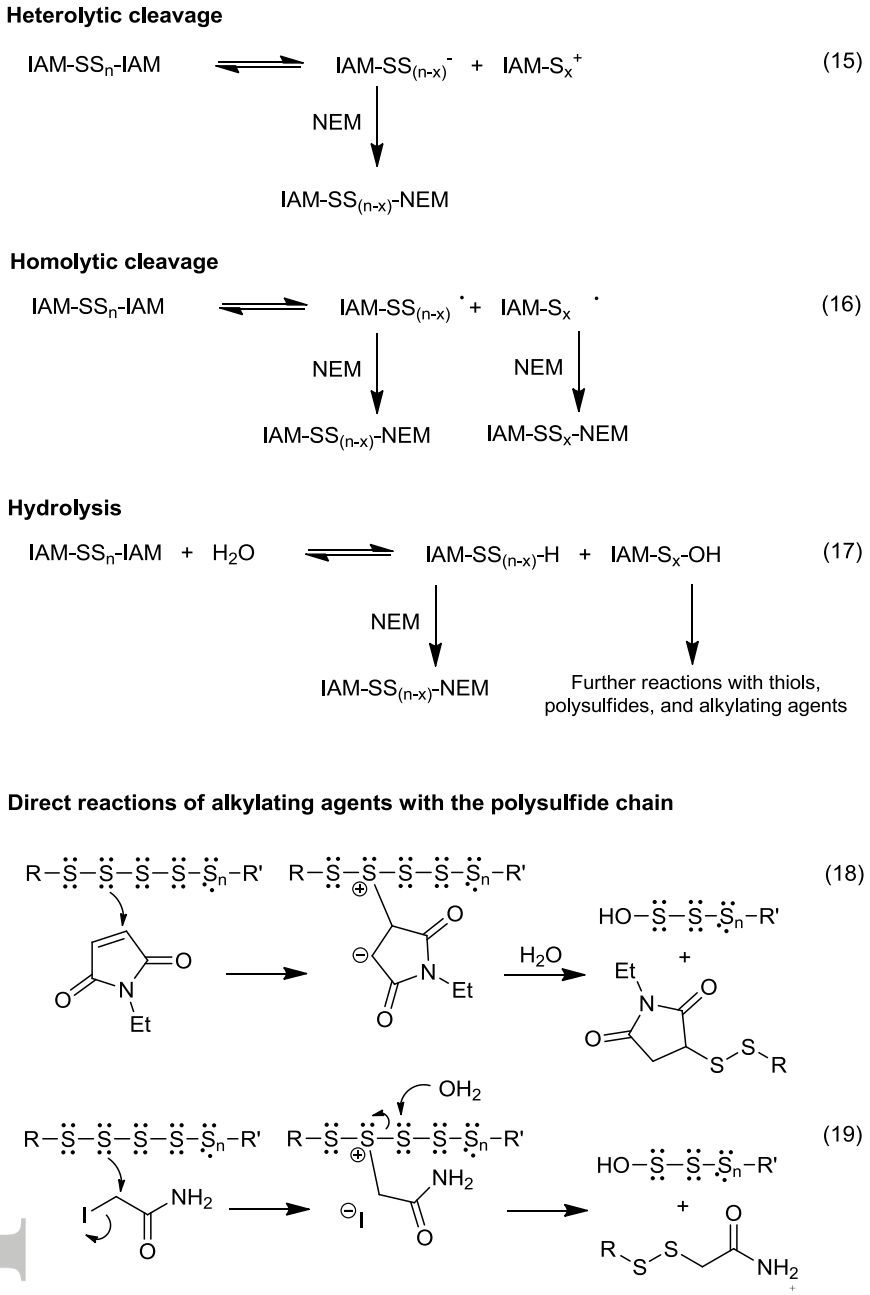

Reactions/mechanisms 15-19: Hypothetical mechanisms for polysulfur chain cleavage promoted by IAM and NEM.

These models warrant further investigation in future studies.

Speciation of cysteine-polysulfide species

Cys and glutathione (GSH) polysulfides were observed to be highly abundant in biological samples including cells and tissue (Ida *et al.*, 2014; Doka *et al.*, 2016; Akaike *et al.*, 2017).

Cys polysulfides were previously demonstrated to form via oxidative posttranslational reactions of either Cys or sulfide. Inorganic polysulfides can oxidize Cys thiols to generate Cys-polysulfide species (Greiner *et al.*, 2013) and oxidized Cys residues can also react with sulfide to form Cys polysulfides (Carballal *et al.*, 2011; Francoleon *et al.*, 2011; Cuevasanta *et al.*, 2015; Nagy, 2015; Vasas *et al.*, 2015). In addition, Cys-polysulfides can be generated by direct enzymatic reactions of CSE and CBS using cystine (Yamanishi & Tuboi, 1981; Ida *et al.*, 2014) as substrate and even more efficiently from Cys by PLP-dependent catalytic reactions of cysteinyl-tRNA synthetase 2 (CARS2) (Akaike *et al.*, 2017) without the involvement of any oxidation reaction or H_2S. It was proposed that organic low molecular weight polysulfides such as Cys and GSH polysulfides can trigger polysulfidation on functional and regulatory protein Cys residues via transsulfuration reactions (beside CARSs-catalyzed co-translational protein polysulfidation (Akaike *et al.*, 2017)) and hence play a major role in polysulfidation-regulated redox signaling events (Ida *et al.*, 2014). Therefore, we investigated whether alkylation of these species in simple aqueous solutions can change speciation via these chemistries.

Cys and GSH polysulfide species were prepared by mixing either the appropriate thiol or disulfide species with sulfide or with an inorganic polysulfide solution (made by dissolving Na_2S_3 or Na_2S_4). Just as in the case of inorganic polysulfide species, we found that the distribution of alkyl polysulfides does not depend on the nature of the reagents used to prepare them. Although for both Cys and GSH, polysulfides containing up to 5 sulfurs could be detected, we only had authentic isotopically labelled internal standards available for the persulfide and trisulfide derivatives, therefore the following quantitative measurements were only considering these species (apart from the corresponding Cys thiol and inorganic sulfide, disulfide and trisulfide species).

Using a recently developed quantitative mass spectrometry method (Akaike *et al.*, 2017) we examined how incubation time and alkylating agent concentration affect speciation of Cys and GSH polysulfides using HPE-IAM, NEM and MBB as representative model compounds. Figure 4 shows that after 3h incubation the concentration of an IAM-based alkylating agent (HPE-IAM) in the 0.5-10 mM range had little effect on the observed speciation of the alkylated Cys and GSH persulfide species (R-SS-HPE-IAM, R = Cys or GSH). However, the alkylated trisulfide concentrations increased with the alkylating agent concentration (except at 0.1 mM, at which concentration the alkylating agent is at a substoichiometric molar ratio compared to the sulfur species). This indicates that speciation

equilibria in solution are indeed affected at the lower alkylating agent concentrations and that alkylation of longer polysulfides is most likely slower compared to the ones containing a shorter chain length. A concomitant drop in the inorganic disulfide species (HS_2^-) was observed in both cases, but the concentration of the inorganic trisulfide (HS_3^-) increased with higher HPE-IAM concentration (Figure 4 C&D). We observed slow changes in speciation over time in the 30 min to 6 h time window, even at the highest alkylating agent excess (10 mM), indicating that HPE-IAM cannot efficiently cleave dialkyl polysulfide chains. This is demonstrated by the time-resolved changes of HPE-IAM alkylated Cys and GSH persulfide species in Figure S5. However, a clear drop can be seen in HPE-IAM-alkylated trisulfide adducts, albeit not nearly as prominent as in the case of NEM (see Figure S6). Therefore, it is likely that at higher concentrations of IAM, Reactions 15-17 and 19 also cause longer polysulfur chain cleavage over longer timescales. Of note, we could account for most of the oxidizing equivalents in both systems.

Next, we conducted a similar experiment using NEM instead of HPE-IAM. As with inorganic polysulfides, we found a strikingly different distribution of the detected sulfur species. Most notably, significantly less R-SS-NEM-derivatives were detected (both for Cys and GSH) compared to when HPE-IAM was used as the alkylating agent; the trisulfide species could not be detected under any conditions (for a comparison see speciation with different alkylating agents after 3h incubation times at 10 mM alkylating agent concentration in Figure 5). Moreover, Cys-persulfide concentrations sharply decreased with increasing NEM concentration as well as at constant NEM over time (Figure 4E and S6A). This observation is consistent with the notion that NEM favours the formation of NEM-alkylated Cys thiol species. Interestingly, neither concentration nor incubation time with NEM had much of an effect on the concentration of the detected NEM-derivatized glutathione-persulfide species (see Figures 4F and S6B), which was notably much larger than the corresponding NEM-alkylated Cys persulfides (compare the middle green bars in Figure 5A and B). This observation indicates that rates and effectiveness of these reactions will very much depend on the nature of the polysulfide species, which introduces another layer of complexity in terms of protein, GSH, Cys and inorganic polysulfide detection in biological systems, where different polysulfide species will likely engage in trans-sulfuration reactions as well.

We repeated these experiments with monobromobimane (MBB), an alkylating agent with fluorescent properties that is often used to detect Cys, GSH and inorganic sulfane sulfur

species in biological systems (Cotgreave & Moldeus, 1986; Ida *et al.*, 2014; Nagy *et al.*, 2014). In addition, MBB has been used widely as a derivatization agent for hydrogen sulfide detection in biological samples (Wintner *et al.*, 2010; Shen *et al.*, 2011). As with HPE-IAM, the concentration of the applied MBB and incubation time had little effect on the detected concentrations of MBB-alkylated Cys and glutathione persulfide, but the concentrations of the corresponding trisulfide species increased with the applied MBB concentration consistent with Curtin-Hammett control over MBB-derivatized sulfur species speciation (Figure S7). However, at higher MBB concentrations a time-resolved decrease in the trisulfide derivative indicated that just like NEM, MBB can also cleave longer dialkyl polysulfide chains; these results suggest that MBB lies inbetween HPE-IAM and NEM in terms of effectiveness to cleave polysulfur chains (see Figure S8B and S8D).

In order to provide biological credence to this observation we investigated the effects of MBB concentration and incubation time on the amount of detected sulfide by the MBB method (Nagy *et al.*, 2014) in human blood serum and plasma. Although under similar conditions the MBB-sulfide reaction is expected to be completed in <10 min (see Figure 6A), a constant increase in the amounts of detected sulfide as a function of incubation time with MBB (as long as up to 1380 min, see Figure 6B) was observed in a concentration-dependent manner (Fig 6B inset). This clearly indicates that MBB can shift the speciation of sulfur species in human serum and plasma and extract sulfide from different biological sulfide pools (see (Nagy *et al.*, 2014)). A previous study found that more sulfide is detected in whole blood when using NEM or MBB compared to when using IAM, which is consistent with our proposal that NEM and MBB can more effectively cleave polysulfur chains than IAM (Sutton et al, 2018).

This phenomenon was further investigated using GAPDH and a recently developed protein polysulfide detection method, PMSA (Akaike *et al.*, 2017), which builds on the observation that NEM can cleave longer dialkyl polysulfide chains. GAPDH was treated with different concentrations of inorganic polysulfide solutions made up using either Na_2S_2 or Na_2S_3 salts. In all cases, a similar Cys polysulfidation pattern was observed indicating that GAPDH is already polysulfidated to a large extent even in the absence of additional polysulfide (Akaike *et al.*, 2017). However, the nature of the alkylating agent also makes a difference in this assay (see Figure 7). As expected, NEM was most efficient in cleaving already alkylated Cys-polysulfide residues on the protein, followed by MBB, and IAM had

no cleaving effect. The fact that NEM and 2-mercaptoethanol or DTNB treatments showed a similar pattern suggests that NEM cleaved all Cys-polysulfide chains on the protein.

If these reactions indeed proceed via one of the mechanisms proposed in reactions 17-19, then this would raise an important issue regarding the common detection of protein sulfenic acids by dimedone trapping (Poole *et al.*, 2004; Paulsen & Carroll, 2013): one could envision that if Cys polysulfide species undergo hydrolysis via a mechanism as outlined in equation 17, than specific trapping of sulfenic acid species would pull the equilibria towards the formation of the hydrolytic products. In addition, the Alk-S_x^+ species that is generated upon heterolytic cleavage of polysulfides (reaction 15) are also expected to rapidly hydrolyze to give the corresponding sulfenic acid derivative (Alk-S_x-OH). Therefore, theoretically these equilibria could also be pulled towards the formation of the hydrolysis products. A corollary of this notion is that a proportion of the detected protein sulfenic acid pool in biological systems might in fact originate from protein polysulfide species instead. We recently proposed that a major fraction of the dimedone-labelled protein pool may represent perthiosulfenic acid derivatives. *Ab initio* calculations suggested that dimedone is not reactive towards polysulfide species, only towards sulfenic, persulfenic or polysulfenic acid derivatives (Heppner *et al.*, 2017), which is consistent with this hypothesis. In order to test these assumptions in a relevant biological context we incubated isolated GAPDH that was pretreated either with inorganic polysulfides, H_2O_2 or left untreated. We detected more dimedone-labelled Cys and Cys polysulfide derivatives on GAPDH Cys residues when the isolated protein was treated with inorganic polysulfides (which is not expected to directly provide Cys-OH) compared to when it was treated with H_2O_2 (which is known to induce Cys-OH on GAPDH) or when it was left untreated (see Fig 8A). When the samples were pretreated with 100 mM IAM the observed amounts of dimedone-labelled Cys derivatives dropped by orders of magnitude (Fig 8B). Based on these results we cannot distinguish at present whether dimedone-labeling was due to hydrolysis of polysulfur chains (analogous to reaction 17) or due to autooxidation of sulfurs in GAPDH-Cys derivatives. The fact that much lower amounts of dimedone labeling were observed when a high concentration of IAM was used prior to capturing Cys-OH with dimedone suggests that the hydrolysis of dialkyl polysulfides may not be very efficient in this case. However, it is also plausible that this high amount of alkylating agent pulled equilibria 15-17 to the right or directly cleaved polysulfide chains via reaction 19. Importantly, these observation do not exclude the possibility that the dimedone adducts were formed by hydrolysis reactions of non-alkylated polysulfides. A

thorough kinetic study to elucidate the mechanism by which polysulfides induce dimedone labelling is required. Taken together, these observations raise the possibility that a fraction of the previously detected sulfenic acid pool, which used dimedone-based molecules as Cys-OH specific capturing agents, could in fact represent polysulfide species.

We also studied GSH-polysulfide speciation by NMR spectroscopy and direct infusion mass spectrometry in the absence of any derivatization. Interestingly, both NMR and ESI-MS analysis indicated that addition of NaSH to disulfides resulted in the formation of corresponding thiol and dialkyl trisulfide species. Initial studies on the equilibrium of H_2S with disulfides were performed using GSSG and ^{1}H-NMR analyses. Figure 9A displays the stacked ^{1}H NMR spectra for GSH (10 mM), GSSG (10 mM), GSSSG (10 mM) and GSSG (10 mM) + NaSH (5 mM), from bottom to top, respectively. As can be seen in Figure 9, addition of 5 mM NaSH to 10 mM GSSG causes the formation of two new species. Comparison of the chemical shifts for these new species with those of authentic standards indicates that the newly formed species are GSH (δ = 4.56 ppm) and GSSSG (δ = 3.16-3.22 and 3.43-3.48 ppm). The ratio of GSH:GSSSG was 2:1, which would be the expected ratio of RSH:RSSSR from the proposed formation of RSSSR, as described below (Reactions 20 and 21). Further addition of NaSH (10 and 15 mM) to 10 mM GSSG causes subsequent increases in the formation of these newly formed species (Figure 9B).

Our NMR analyses indicate that addition of NaSH to GSSG induces formation of thiol and dialkyl trisulfide species after equilibration. Therefore, it became of interest to confirm the presence of thiol and dialkyl trisulfide species by ESI-MS analyses. The ESI-MS spectra of equilibrated samples (30 min) of both 1 mM GSSG + 0.5 mM NaSH are displayed in Figure 9C, confirming that addition of NaSH to GSSG causes formation of the corresponding thiol (Figure 9D, m/z = 307.98) and trisulfide species (Figure 9D, m/z = 645.09), which are not present in samples of GSSG alone (Figure 9C).

It has been widely accepted that the initial reaction of H_2S with disulfides results in an equilibrated mixture with corresponding thiol and persulfide species (Francoleon *et al.*, 2011; Vasas *et al.*, 2015) (Reaction 20).

$$H_2S + RSSR \rightleftharpoons RSSH + RSH \qquad (20)$$

It has to be noted that these reactions likely proceed via nucleophilic attack by an anionic species (HS^- or RSS^-) rather than by H_2S directly, but for the sake of simplicity the charged states of the reactants/products are not depicted here. Lack of detection of persulfide species in the equilibrated systems described above implies that formed persulfide species are subject to further reaction under the studied conditions. This is also consistent with the detection of dialkyl trisulfide species by both NMR and ESI-MS analysis. It is therefore reasonable to consider that persulfides participate in a second equilibrium that results in dialkyl trisulfide formation (Reaction 21).

$$RSSH + RSSR \rightleftharpoons RSSSR + RSH \qquad (21)$$

We previously studied the reaction of cystine (CysSSCys) with sulfide using ^{1}H NMR spectroscopy, in which we observed the formation of two distinct Cys derivatives (other than the thiol and disulfide species), which were tentatively assigned to be Cys-persulfide (CysSSH) and the dialkyl trisulfide (CysSSSCys) (Vasas *et al.*, 2015). This corroborates the proposed model (see reactions 20 and 21), in which persulfides indeed form as intermediate species in the reactions of GSSG with sulfide to finally give GSSSG. We argued that speciation equilibria can favor very different distribution of sulfur species in a system specific manner (Vasas *et al.*, 2015), which is consistent with the observed differences in the CysSSCys and GSSG systems.

We here would like to refer the reader to our companion paper, where we demonstrated that equilibrium 21 is indeed likely to prevail in cellular systems. We found that cysteine trisulfide (Cys-SSS-Cys) provide a useful pharmacological tool because treatment of cells with this dialkyl trisulfide results in high intracellular levels of hydropersulfides (due to a shift towards the backward reaction of reaction 21), which protected HEK293T cells from electrophilic stress (Bianco *et al.*, 2018).

Furthermore, if indeed a highly nucleophilic persulfide is fleeting in the case of the GSH system due to subsequent reaction with electrophilic species present in the reaction mixture (e.g. a disulfide, Reaction 21), it is expected that dialkyl trisulfide formation could be avoided or lessened by the presence of an alternate electrophilic species capable of trapping the intermediate RSSH (Reaction 22). In other words, trapping of RSSH by an exogenous electrophile (Reaction 22) would be competitive with trapping of RSSH by RSSR (Reaction 21).

$$RSSH + E^+ \rightarrow RSS\text{-}E + H^+ \quad (E^+ = \text{electrophile}) \quad (22)$$

Consequently, increasing concentrations of exogenous electrophile would be expected to cause a leftward shift in the equilibrium of Reaction 21, because persulfides are expected to act as better nucleophiles compared to the corresponding thiols (especially at physiological pH where the GSH thiol is mostly protonated and the persulfide is likely in its more nucleophilic perthiolate form) and hence react faster with the alkylating agent. This would limit dialkyl trisulfide formation. Indeed, addition of increasing concentrations of IAM (0.5-2.5 mM) to equilibrated mixtures of 10 mM GSSG + 5 mM NaSH caused subsequent decreases in the concentration of GSSSG (δ = 3.16-3.22 and 3.43-3.48 ppm, Figure 9E). Additionally, use of the electrophile NEM (0-2.5 mM) as a trap for the intermediate GSSH displayed similar reactivity to that of IAM (0-2.5 mM), ultimately leading to decreased amounts of GSSSG upon increasing addition of NEM (Figure 9F). This also indicates that IAM acts as a better trap for GSSH, in comparison to NEM, suggesting that GSSH preferentially reacts with GSSG in the presence of NEM, but not in the presence of IAM (note: the nucleophilicity of polysulfides increases with increasing sulfur chain length;(Nagy, 2015) however, no direct reaction between GSSSG and IAM was observed under the studied conditions.)

Taken together, the above data indicate that exogenously added electrophilic species compete with disulfides for the trapping of persulfides. To further verify this, the products formed after addition of 0.5 mM IAM to equilibrated samples of GSSG + 0.5 mM NaSH were analyzed using ESI-MS. Addition of IAM to an equilibrated solution of GSSG + NaSH (Figure 9E) traps GSSH, again shifting the equilibrium away from GSSSG (Reaction 21), and resulting in the carboxamidomethylated-GSSH species ($[GSS+AM+H]^+$, m/z = 397.19, Figure 9G).

Alternatively, some of the detected alkylated Cys-polysulfide species could also originate from dialkyl polysulfides via similar mechanisms that are outlined in reaction 17 for alkylated inorganic polysulfides.

Speciation of polysulfide species in organic media

Up to this juncture, using aqueous model systems of likely relevance for cellular events occurring either in the cytosol or in extracellular fluids, we have demonstrated that alkylation of inorganic-, Cys-, GSH- and protein-polysulfides can dramatically change the distribution of polysulfur species with different chain lengths. However, a significant part of the biological chemistry pertinent to sensing, signal transduction and adjustment of cellular function takes place in more lipophilic compartments such as the cell membrane or cellular organelles. We were therefore interested to see whether some of the key findings observed also apply to non-aqueous systems.

Mixing NBu_4SH, an organic soluble source of hydrosulfide, with elemental sulfur (S_8) produces inorganic polysulfides in organic solution (Bailey *et al.*, 2016). The fact that polysulfide species are brightly, and differentially, colored in organic solvents presents a unique opportunity to assess differences in speciation before and after quenching with benzyl chloride.

$S_2^{\bullet-}$, $S_3^{\bullet-}$ and $S_4^{\bullet-}$ have UV-Vis absorbances in the visible region in electron-pair-donating solvents and are yellow (400 nm), blue (620 nm), and red (520 nm), respectively (although $S_2^{\bullet-}$ absorbance was observed in a KI matrix and the absorption attributed the $S_4^{\bullet-}$ is the subject of some debate) (Chivers & Drummond, 1972; Chivers & Elder, 2013). In our UV-Vis experiments, similar speciation was observed across the 1:1, 1:2, and 1:3 ratios, with the $S_4^{\bullet-}$ (490 nm) being the predominant species at room temperature (see Figure 10A-C). Importantly, as the temperature was increased, more of the $S_3^{\bullet-}$ (610 nm) was formed. For the 1:8 ratio system (see Figure 10D), the predominant species at room temperature was $S_2^{\bullet-}$ (426 nm) and with further increase in temperature the equilibrium was shifted towards to formation of more $S_3^{\bullet-}$ (610 nm). The fact that the transitions between temperatures were completely reversible in all cases nicely demonstrates that we are indeed looking at true shifts in speciation equilibria. These experiments demonstrated that for any given ratio, the speciation of organic polysulfides is very sensitive to temperature.

Next, we compared the solution speciation observed in the UV-Vis spectra to the speciation of dibenzyl polysulfides (Bn_2S_X) after quenching these solutions with the electrophile benzyl chloride (see reaction 23) using ^1H NMR integration values of the benzyl proton resonances (see Table 2). Benzyl chloride was used as a trapping agent due to the well-characterized chemical shifts of the different benzyl polysulfide products and prior use to identify polysulfides (Ahrika *et al.*, 1999; Bailey & Pluth, 2015).

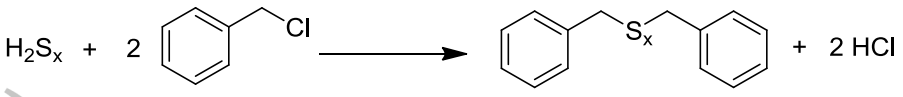

(23)

The ^{1}H-NMR spectra showed the trapping of dibenzyl trisulfide (Bn_2S_3), dibenzyl tetrasulfide (Bn_2S_4), and dibenzyl pentasulfide (Bn_2S_5). Dibenzyl disulfide (Bn_2S_2) was only observed in the 1:8 S_8:NBu_4SH ratio system. The relative molar ratio of the benzyl trapped polysulfides (Bn_2S_3:Bn_2S_4:Bn_2S_5) was conserved across all 1:X S_8: NBu_4SH where $X \leq 4$. This trend deviates for the 1:8 S_8: NBu_4SH system as would be expected based on the UV-Vis data. Importantly, in contrast to the observed temperature dependence in the UV-Vis spectra, changing the temperature in the 1:2 S_8: NBu_4SH ratio system followed by electrophilic quenching of polysulfide species had no effect on the observed Bn_2S_3:Bn_2S_4:Bn_2S_5 ratio across all three temperature points.

Taken together, these results confirm our hypothesis that the electrophilic quenching of a mixed polysulfide system is under Curtin-Hammett control; meaning that in this system the reactive polysulfides are rapidly interconverting on a much shorter timescale compared to the reaction with benzyl chloride (reaction 23). As such, the relative alkyl polysulfide product ratios are merely a reflection of the relative rates of reaction with benzyl chloride (and other electrophiles) and do not report on the solution speciation.

Implications for the detection of sulfur species in biological systems

Reactive sulfur species are emerging as part of a possibly vestigial chemistry that governs contemporary cell biology (Cortese-Krott *et al.*, 2017). The particular chemical properties of sulfur, including its ability to transfer electrons and form chains of variable length (catenation tendency), play an important role in enabling the sulfhydryl moiety of reactive cysteine residues to fulfil important functions in redox regulatory processes. Consequently, a large body of literature exists related to the different redox and electrophilic Cys modifications in the context of oxidative stress and redox regulation of cell signaling (Rudolph & Freeman, 2009; Nagy & Winterbourn, 2010b). Per/polysulfide formation on protein Cys residues represents a relatively new concept in redox biology, and a number of different research groups have shown that protein polysulfide species are abundant in cells and tissues with important biological functions (Mustafa *et al.*, 2009; Ida *et al.*, 2014; Zhang *et al.*, 2014; Gao *et al.*, 2015; Doka *et al.*, 2016; Longen *et al.*, 2016; Akaike *et al.*, 2017). Moreover, these

species are not only generated by posttranslational events but also form translationally, giving credence to their pivotal biological role (Akaike *et al.*, 2017).

Tools to study polysulfidation and other redox modifications of protein Cys residues have been available for some time now and will be developed further and refined in the years to come. However, as we show in this contribution, the gold standard alkylation-based protocols can have serious caveats, and in many cases the actual readouts do not necessarily represent true cellular speciation of Cys derivatives. Our data indicates that methods using NEM or MBB based alkylation strategies will either detect lower levels or completely miss the existence of per/polysulfide species compared to IAM-based alkylation protocols. On the other hand, methodologies that are designed to detect protein disulfides will benefit from faster alkylation of sulfhydryl groups by NEM compared to IAM by avoiding artifactual oxidation. Furthermore, our data indicate that sulfide concentrations in clinical samples determined using the MBB method should be interpreted with caution, keeping in mind that measured concentrations involve not only sulfide but also different proportions (depending on the experimental conditions) of the bound sulfane sulfur pool. Reporting "free sulfide levels" with this method should therefore be avoided.

Our results also indicate that although dimedone labeling is specific to sulfenic acid residues, due to shifting speciation equilibria (e.g. in this case reaction 17) can result in overestimation of Cys-OH species, and a fraction of the previously assigned sulfenic acid pool could in fact represent polysulfide species. Therefore, alkylating agents that are specific to a particular Cys derivative, like dimedone, need to be used with care because they, too, can pull speciation equlilibria into one direction.

We caution that the chemistries discussed in the present body of work should not be neglected in studies addressing the chemical biology of Cys modifications. In the context of endogenous polysulfide detection, it will be of relevance to not only posttranslational protein modification processes (and therefore in adjusting protein function at the level of cysteine moieties) downstream of cellular hydrogen sulfide production, but also to events upstream by generating sulfur equivalents with distinct redox properties from organic per/polysufides. Given the dynamic nature of this 'sulfur redox metabolome' identifying specific regulatory events with specific sulfur species will remain a formidable challenge in the years to come. Given the outstanding physiological relevance and clinical potential of redox-based cellular

signaling events (Cortese-Krott *et al.*, 2017) we do not intend to suggest that all current state-of-the-art protocols give rise to inadequate conclusions, but we urge the community to interpret their results with modesty, keeping in mind the limitations of the corresponding techniques. For example, measured "free sulfide levels" and definitive designation of effector sulfur species should be handled with extraordinary care.

Footnotes

[1] From now on we will use the term sulfide to refer to the sum of its different protonated forms that exist in solution, i.e. H_2S, HS^- and S^{2-}.

[2] Sulfane sulfur species are oxidized derivatives of sulfide, which contain sulfur(s) at the zero valent oxidation state.

Acknowledgments

Financial support from the National Research, Development and Innovation Office (grants No.: KH17_126766 and K 109843) and the National Institute for Health (grant No.: R21AG055022-01) for P.N. is acknowledged. P.N. was a János Bolyai Research Scholar of the Hungarian Academy of Sciences. Financial supports from the National Science foundation (grant No.: CHE-1454747 and CHE-1566065) to M.D.P and J.P.T are also acknowledged. This work was supported in part by Grants-in-Aid for Scientific Research (25253020, and 16K15208 to T.A.) and a Grant-in-Aid for Scientific Research on Innovative Areas (26111008, 26111001, and 15K21759 to T.A.) from the Ministry of Education, Sciences, Sports and Technology (MEXT), Japan.

Competing Interests Statement: None.

References

Ahrika A, Robert J, Anouti M, Paris J (1999). Nucleophilic substitution of alkyl halides by electrogenerated polysulfide ions in N,N-dimethylacetamide. Acta Chem Scand 53**:** 513-520.

Akaike T, Ida T, Wei FY, Nishida M, Kumagai Y, Alam MM*, et al.* (2017). Cysteinyl-tRNA synthetase governs cysteine polysulfidation and mitochondrial bioenergetics. Nat Commun 8**:** 1177.

Bailey TS, Pluth MD (2015). Reactions of isolated persulfides provide insights into the interplay between H2S and persulfide reactivity. Free Radical Biol Med 89**:** 662-667.

Bailey TS, Henthorn HA, Pluth MD (2016). The Intersection of NO and H2S: Persulfides Generate NO from Nitrite through Polysulfide Formation. Inorg Chem 55**:** 12618-12625.

Berzelius J (1822). De la Composition des Sulfures Alcalins. Ann Chim Phys 20**:** 113-141.

Bianco CL, Akaike T, Ida T, Nagy P, Toscano JP, Kumagai Y*, et al.* (2018). The Reaction of Hydrogen Sulfide with Disulfides: Formation of a Stable Trisulfide and Implications to Biological Systems. Br J Pharmacol conditionally accepted.

Bostelaar T, Vitvitsky V, Kumutima J, Lewis BE, Yadav PK, Brunold TC*, et al.* (2016). Hydrogen Sulfide Oxidation by Myoglobin. J Am Chem Soc 138**:** 8476-8488.

Bouillaud F, Blachier F (2011). Mitochondria and sulfide: a very old story of poisoning, feeding, and signaling? Antioxid Redox Signal 15**:** 379-391.

Boulegue J, Michard G (1978). Constantes de formation des ions polysulfures S-26, S-25 et S-24 en phase aqueuse. J Fr Hydrol 9**:** 24-33.

Carballal S, Trujillo M, Cuevasanta E, Bartesaghi S, Moller MN, Folkes LK*, et al.* (2011). Reactivity of hydrogen sulfide with peroxynitrite and other oxidants of biological interest. Free Radic Biol Med 50**:** 196-205.

Chivers T, Drummond I (1972). Characterization of the trisulfur radical anion S3- in blue solutions of alkali polysulfides in hexamethylphosphoramide. Inorg Chem 11**:** 2525-2527.

Chivers T, Elder PJ (2013). Ubiquitous trisulfur radical anion: fundamentals and applications in materials science, electrochemistry, analytical chemistry and geochemistry. Chem Soc Rev 42**:** 5996-6005.

Cloke PL (1963). The geologic role of polysulfides—Part I The distribution of ionic species in aqueous sodium polysulfide solutions. Geochim Cosmochim Acta 27**:** 1265-1298.

Cortese-Krott MM, Koning A, Kuhnle GGC, Nagy P, Bianco CL, Pasch A*, et al.* (2017). The Reactive Species Interactome: Evolutionary Emergence, Biological Significance, and Opportunities for Redox Metabolomics and Personalized Medicine. Antioxid Redox Signal 27**:** 684-712.

Cortese-Krott MM, Kuhnle GG, Dyson A, Fernandez BO, Grman M, DuMond JF*, et al.* (2015). Key bioactive reaction products of the NO/H_2S interaction are S/N-hybrid species, polysulfides, and nitroxyl. P Natl Acad Sci USA 112**:** E4651-4660.

Cotgreave IA, Moldeus P (1986). Methodologies for the application of monobromobimane to the simultaneous analysis of soluble and protein thiol components of biological systems. J Biochem Biophys Methods 13**:** 231-249.

Cuevasanta E, Lange M, Bonanata J, Coitino EL, Ferrer-Sueta G, Filipovic MR*, et al.* (2015). Reaction of Hydrogen Sulfide with Disulfide and Sulfenic Acid to Form the Strongly Nucleophilic Persulfide. J Biol Chem 290**:** 26866-26880.

Doka E, Arner ESJ, Schmidt EE, Nagy P (2017). ProPerDP, a Protein Persulfide Detection Protocol. In: Beltowski J (ed). *Methods Mol Biol*, edn, Vol. Special Issue: Springer, in press. p^pp.

Doka E, Pader I, Biro A, Johansson K, Cheng Q, Ballago K*, et al.* (2016). A novel persulfide detection method reveals protein persulfide- and polysulfide-reducing functions of thioredoxin and glutathione systems. Sci Adv 2**:** e1500968.

Donohue J (1961). Chapter 1 - the structures of elemental sulfur† a2 - kharasch, n. In. *Organic Sulfur Compounds*, edn: Pergamon. p^pp 1-6.

Francoleon NE, Carrington SJ, Fukuto JM (2011). The reaction of H(2)S with oxidized thiols: generation of persulfides and implications to H(2)S biology. Arch Biochem Biophys 516**:** 146-153.

Gao XH, Krokowski D, Guan BJ, Bederman I, Majumder M, Parisien M*, et al.* (2015). Quantitative H2S-mediated protein sulfhydration reveals metabolic reprogramming during the integrated stress response. Elife 4**:** e10067.

Garai D, Rios-Gonzalez BB, Furtmuller PG, Fukuto JM, Xian M, Lopez-Garriga J*, et al.* (2017). Mechanisms of myeloperoxidase catalyzed oxidation of H2S by H2O2 or O2 to produce potent protein Cys-polysulfide-inducing species. Free Radic Biol Med 113**:** 551-563.

Giggenbach W (1972). Optical spectra and equilibrium distribution of polysulfide ions in aqueous solution at 20.deg. Inorg Chem 11**:** 1201-1207.

Greiner R, Palinkas Z, Basell K, Becher D, Antelmann H, Nagy P*, et al.* (2013). Polysulfides link H_2S to protein thiol oxidation. Antioxid Redox Signal 19**:** 1749-1765.

Gun J, Modestov AD, Kamyshny A, Ryzkov D, Gitis V, Goifman A*, et al.* (2004). Electrospray ionization mass spectrometric analysis of aqueous polysulfide solutions. Microchim Acta 146**:** 229-237.

Hartle MD, Meininger DJ, Zakharov LN, Tonzetich ZJ, Pluth MD (2015). NBu4SH provides a convenient source of HS(-) soluble in organic solution for H2S and anion-binding research. Dalton Trans 44**:** 19782-19785.

Heppner DE, Hristova M, Ida T, Mijuskovic A, Dustin CM, Bogdandi V*, et al.* (2017). Cysteine perthiosulfenic acid (Cys-SSOH): A novel intermediate in thiol-based redox signaling? Redox Biol 14**:** 379-385.

Ida T, Sawa T, Ihara H, Tsuchiya Y, Watanabe Y, Kumagai Y*, et al.* (2014). Reactive cysteine persulfides and S-polythiolation regulate oxidative stress and redox signaling. P Natl Acad Sci USA 111**:** 7606-7611.

Jackson MR, Melideo SL, Jorns MS (2012). Human sulfide:quinone oxidoreductase catalyzes the first step in hydrogen sulfide metabolism and produces a sulfane sulfur metabolite. Biochemistry 51**:** 6804-6815.

Jung M, Kasamatsu S, Matsunaga T, Akashi S, Ono K, Nishimura A*, et al.* (2016). Protein polysulfidation-dependent persulfide dioxygenase activity of ethylmalonic encephalopathy protein 1. Biochem Biophys Res Commun 480**:** 180-186.

Kamyshny A, Borkenstein CG, Ferdelman TG (2009). Protocol for Quantitative Detection of Elemental Sulfur and Polysulfide Zero-Valent Sulfur Distribution in Natural Aquatic Samples. Geostand Geoanal Res 33**:** 415-435.

Kamyshny A, Jr., Ekeltchik I, Gun J, Lev O (2006). Method for the determination of inorganic polysulfide distribution in aquatic systems. Anal Chem 78**:** 2631-2639.

Kamyshny A, Jr., Goifman A, Gun J, Rizkov D, Lev O (2004). Equilibrium distribution of polysulfide ions in aqueous solutions at 25 degrees C: a new approach for the study of polysulfides' equilibria. Environ Sci Technol 38**:** 6633-6644.

Kamyshny A, Jr., Gun J, Rizkov D, Voitsekovski T, Lev O (2007). Equilibrium distribution of polysulfide ions in aqueous solutions at different temperatures by rapid single phase derivatization. Environ Sci Technol 41**:** 2395-2400.

Kevil C, Cortese-Krott MM, Nagy P, Papapetropoulos A, Feelisch M, Szabo C (2017). Chapter 5 - Cooperative Interactions Between NO and H2S: Chemistry, Biology, Physiology, Pathophysiology A2 - Ignarro, Louis J. In: Freeman BA (ed). *Nitric Oxide (Third Edition)*, edn: Academic Press. p^pp 57-83.

Kimura H (2017). Hydrogen Sulfide and Polysulfide Signaling. Antioxid Redox Signal 27**:** 619-621.

Kumar MR, Farmer PJ (2018). Chemical trapping and characterization of small oxoacids of sulfur (SOS) generated in aqueous oxidations of H2S. Redox Biol 14**:** 485-491.

Kumar V, Kleffmann T, Hampton MB, Cannell MB, Winterbourn CC (2013). Redox proteomics of thiol proteins in mouse heart during ischemia/reperfusion using ICAT reagents and mass spectrometry. Free Radic Biol Med 58**:** 109-117.

Licht S (1987). A Description of Energy-Conversion in Photoelectrochemical Solar-Cells. Nature 330**:** 148-151.

Licht S, Hodes G, Manassen J (1986). Numerical-Analysis of Aqueous Polysulfide Solutions and Its Application to Cadmium Chalcogenide Polysulfide Photoelectrochemical Solar-Cells. Inorg Chem 25**:** 2486-2489.

Longen S, Richter F, Kohler Y, Wittig I, Beck KF, Pfeilschifter J (2016). Quantitative Persulfide Site Identification (qPerS-SID) Reveals Protein Targets of H2S Releasing Donors in Mammalian Cells. Sci Rep 6.

Maronny G (1959). Constantes de dissociation de l'hydrogène sulfuré. Electrochimica Acta 1**:** 58-69.

Mishanina TV, Libiad M, Banerjee R (2015). Biogenesis of reactive sulfur species for signaling by hydrogen sulfide oxidation pathways. Nat Chem Biol 11**:** 457-464.

Miyamoto R, Koike S, Takano Y, Shibuya N, Kimura Y, Hanaoka K*, et al.* (2017). Polysulfides (H2Sn) produced from the interaction of hydrogen sulfide (H2S) and nitric oxide (NO) activate TRPA1 channels. Sci Rep 7**:** 45995.

Modis K, Bos EM, Calzia E, van Goor H, Coletta C, Papapetropoulos A*, et al.* (2014). Regulation of mitochondrial bioenergetic function by hydrogen sulfide. Part II. Pathophysiological and therapeutic aspects. Br J Pharmacol 171**:** 2123-2146.

Mustafa AK, Gadalla MM, Sen N, Kim S, Mu W, Gazi SK*, et al.* (2009). H2S signals through protein S-sulfhydration. Sci Signal 2**:** ra72.

Nagy P (2015). Mechanistic chemical perspective of hydrogen sulfide signaling. Methods Enzymol 554**:** 3-29.

Nagy P, Ashby MT (2007). Reactive sulfur species: kinetics and mechanisms of the oxidation of cysteine by hypohalous acid to give cysteine sulfenic acid. J Am Chem Soc 129**:** 14082-14091.

Nagy P, Winterbourn CC (2010a). Rapid reaction of hydrogen sulfide with the neutrophil oxidant hypochlorous acid to generate polysulfides. Chem Res Toxicol 23**:** 1541-1543.

Nagy P, Winterbourn CC (2010b). Redox chemistry of biological thiols. In: *Advances in Molecular Toxicology* Vol. 4, pp 183-222.

Nagy P, Palinkas Z, Nagy A, Budai B, Toth I, Vasas A (2014). Chemical aspects of hydrogen sulfide measurements in physiological samples. Biochim Biophys Acta 1840**:** 876-891.

Olson KR, Gao Y, DeLeon ER, Arif M, Arif F, Arora N*, et al.* (2017). Catalase as a sulfide-sulfur oxido-reductase: An ancient (and modern?) regulator of reactive sulfur species (RSS). Redox Biol 12**:** 325-339.

Ono K, Akaike T, Sawa T, Kumagai Y, Wink DA, Tantillo DJ*, et al.* (2014). Redox chemistry and chemical biology of H_2S, hydropersulfides, and derived species: implications of their possible biological activity and utility. Free Radic Biol Med 77**:** 82-94.

Padovani D, Hessani A, Castillo FT, Liot G, Andriamihaja M, Lan A*, et al.* (2016). Sulfheme formation during homocysteine S-oxygenation by catalase in cancers and neurodegenerative diseases. Nat Commun 7**:** 13386.

Palinkas Z, Furtmuller PG, Nagy A, Jakopitsch C, Pirker KF, Magierowski M*, et al.* (2015). Interactions of hydrogen sulfide with myeloperoxidase. Br J Pharmacol 172**:** 1516-1532

Paul BD, Snyder SH (2012). H_2S signalling through protein sulfhydration and beyond. Nat Rev Mol Cell Biol 13**:** 499-507.

Paulsen CE, Carroll KS (2013). Cysteine-mediated redox signaling: chemistry, biology, and tools for discovery. Chem Rev 113**:** 4633-4679.

Poole LB, Karplus PA, Claiborne A (2004). Protein sulfenic acids in redox signaling. Annu Rev Pharmacol Toxicol 44**:** 325-347.

Powell MA, Somero GN (1986). Hydrogen-Sulfide Oxidation Is Coupled to Oxidative-Phosphorylation in Mitochondria of Solemya-Reidi. Science 233**:** 563-566.

Rudolph TK, Freeman BA (2009). Transduction of redox signaling by electrophile-protein reactions. Sci Signal 2**:** re7.

Scheele CW (1777). Chemische Abhandlung von der Luft und der Feuer, Upsala und Leipzig. 153.

Seeman JI (1986). The Curtin-Hammett principle and the Winstein-Holness equation: new definition and recent extensions to classical concepts. J Chem Educ 63**:** 42.

Shen XG, Pattillo CB, Pardue S, Bir SC, Wang R, Kevil CG (2011). Measurement of plasma hydrogen sulfide in vivo and in vitro. Free Radical Biol Med 50**:** 1021-1031.

Sobotta MC, Barata AG, Schmidt U, Mueller S, Millonig G, Dick TP (2013). Exposing cells to H2O2: A quantitative comparison between continuous low-dose and one-time high-dose treatments. Free Radical Biol Med 60**:** 325-335.

Steudel R (2003a). Inorganic polysulfides S-n(2-) and radical anions S-n(center dot-). Top Curr Chem 231**:** 127-152.

Steudel R (2003b). Inorganic polysulfanes H2Sn with n > 1. Top Curr Chem 231**:** 99-125.

Sutton T, Minnion M, Barbarino F, Koster G, Bernadette, O Fernandez*, et al.* (2018). A robust and versatile mass spectrometry platform for comprehensive

assessment of the thiol redox metabolome. Redox Biol under review.

Szabo C, Ransy C, Modis K, Andriamihaja M, Murghes B, Coletta C*, et al.* (2014). Regulation of mitochondrial bioenergetic function by hydrogen sulfide. Part I. Biochemical and physiological mechanisms. Br J Pharmacol 171**:** 2099-2122.

Toohey JI (2011). Sulfur signaling: Is the agent sulfide or sulfane? Anal Biochem 413**:** 1-7.

Vasas A, Doka E, Fabian I, Nagy P (2015). Kinetic and thermodynamic studies on the disulfide-bond reducing potential of hydrogen sulfide. Nitric oxide : biology and chemistry / official journal of the Nitric Oxide Society 46**:** 93-101.

Vitvitsky V, Yadav PK, An S, Seravalli J, Cho US, Banerjee R (2017). Structural and Mechanistic Insights into Hemoglobin-catalyzed Hydrogen Sulfide Oxidation and the Fate of Polysulfide Products. J Biol Chem 292**:** 5584-5592.

Wintner EA, Deckwerth TL, Langston W, Bengtsson A, Leviten D, Hill P*, et al.* (2010). A monobromobimane-based assay to measure the pharmacokinetic profile of reactive sulphide species in blood. Br J Pharmacol 160**:** 941-957.

Yamanishi T, Tuboi S (1981). The mechanism of the L-cystine cleavage reaction catalyzed by rat liver gamma-cystathionase. J Biochem 89**:** 1913-1921.

Zhang D, Macinkovic I, Devarie-Baez NO, Pan J, Park CM, Carroll KS*, et al.* (2014). Detection of protein S-sulfhydration by a tag-switch technique. Angew Chem Int Ed Engl 53**:** 575-581.

Figure 1

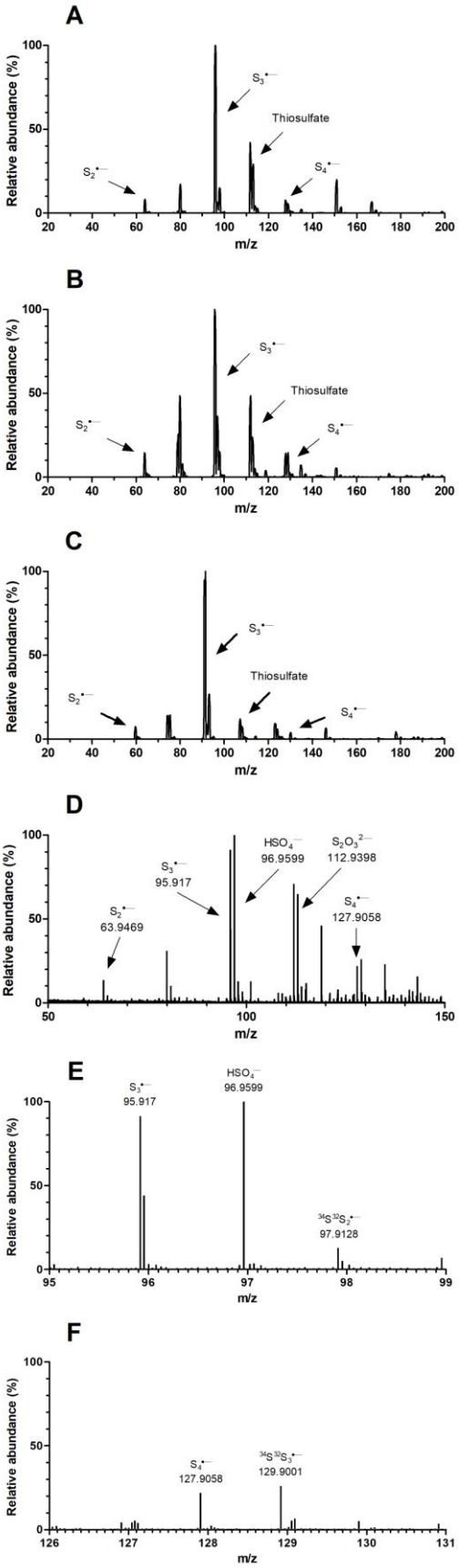

Figure 1: Direct infusion mass spectrometry based detection of inorganic polysulfide speciation in water. Spectra A-C were collected using a Xevo TQ-S detector. Polysulfide solutions were prepared from different polysulfide salts: **A)** Mixed potassium polysulfide (K_2S_x), **B)** Sodium trisulfide (Na_2S_3), **C)** Sodium tetrasulfide (Na_2S_4). Calculated polysulfide m/z are as follows: $S_2^{\bullet-}$ 63.9, $S_3^{\bullet-}$ 95.9 and $S_4^{\bullet-}$ 127.7 and measured m/z varies slightly due to low resolution of the mass spectrometer. Spectra D-F were collected using a Waters SYNAPT G2-Si ESI-ToF-MS high-resolution mass spectrometer. **D**) Full spectrum of potassium polsulfide (K_2S_x) in water shows $S_2^{\bullet-}$, $S_3^{\bullet-}$ and $S_4^{\bullet-}$ radical anions and thiosulfate. **E** and **F**) Zoomed scan spectra of $S_3^{\bullet-}$ and $S_4^{\bullet-}$ radical anion peaks and their associated +2 isotope peaks, respectively. Conditions: T= 20^{o}C, pH=7.4 (ammonium-phosphate buffer), 100 µM polysulfide solutions, 8 µl/min, one scan/sec for one minute. All spectra were recorded in negative ionization mode. Figures are representative of n = 4, 2, 4, 5, 5 and 5 experiments with similar results that were conducted under identical conditions for A, B, C, D, E and F respectively.

Figure 2

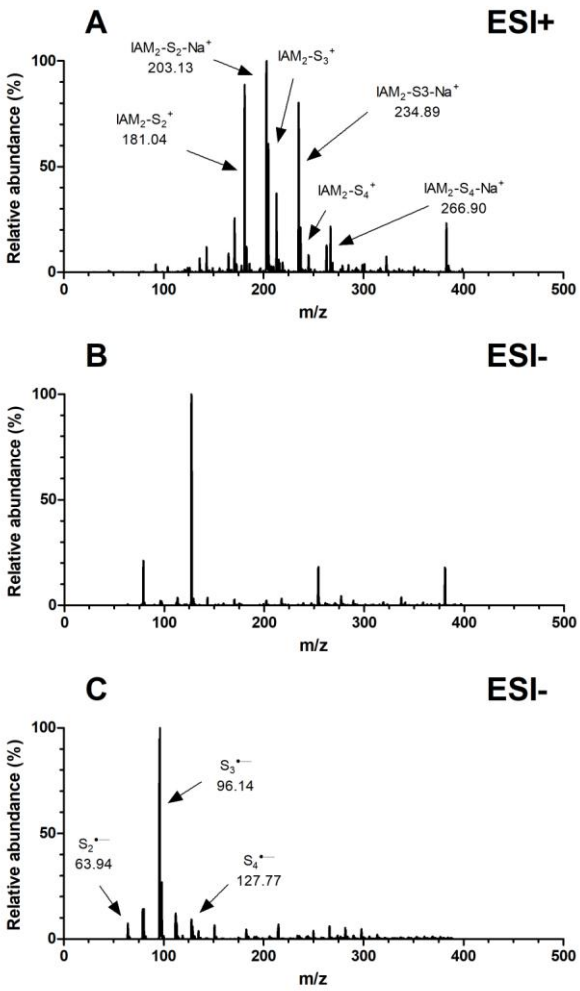

Figure 2: Direct infusion mass spectrometry based detection of inorganic polysulfide species in water before (C) and after addition of IAM (A and B). **B** Shows the absence of polysulfide peaks in negative ionisation mode whilst **A** shows the presence of derivatized polysulfide species (and sodiated peaks) in positive ionisation mode after 10 min incubation of the polysulfide solutions with the alkylating agent.

Conditions: T= 20^{o}C, pH=7.4 (ammonium-phosphate buffer), 100 µM polysulfide solutions, 100 mM IAM, 8 µl/min, one scan/sec for one minute. Spectra are representative of n = 4 experiments that were conducted under identical conditions for A, B and C.

Figure 3 A,B

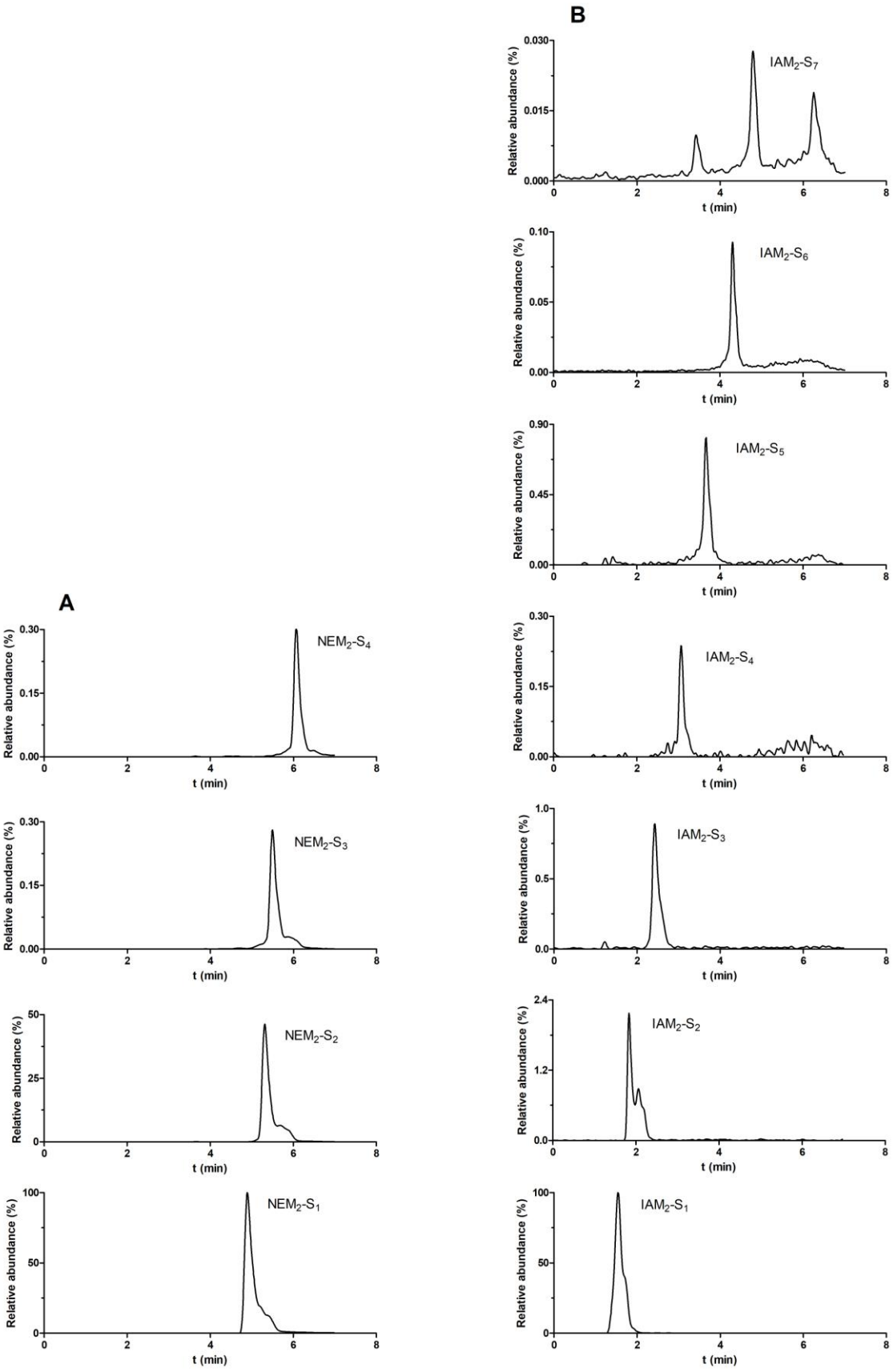

Figure 3 C, D, E, F

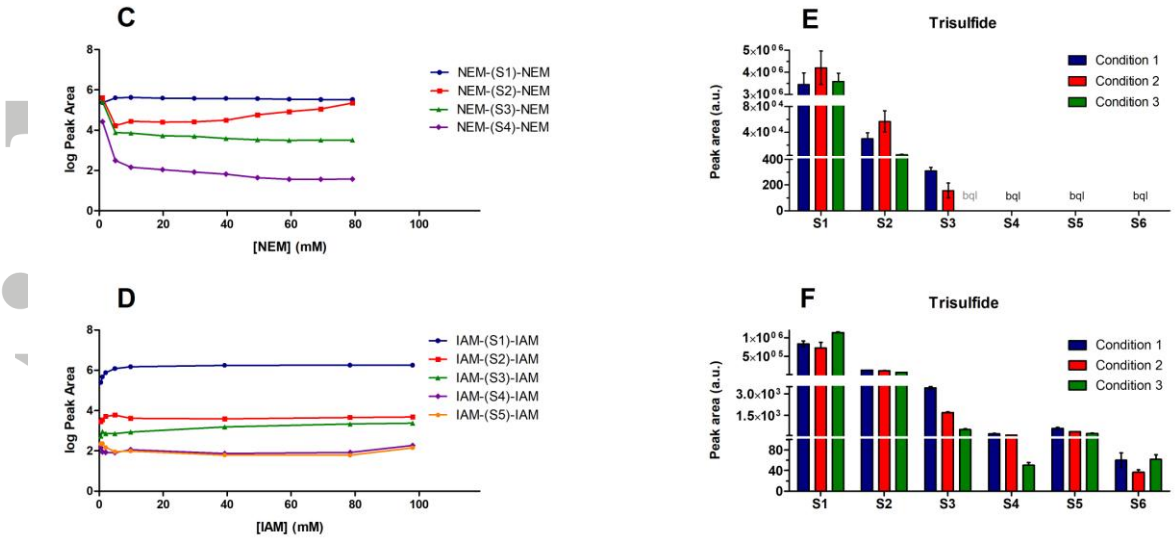

Figure 3: UHPLC-MS detection of alkylated inorganic polysulfides A) Exemplary chromatograms for NEM-derivatized polysulfides in stacked view, in the order of increasing sulfurs from S_1 at the bottom to S_4 at the top **B**) Exemplary chromatograms for IAM-derivatized polysulfides in stacked view, in order of increasing sulfurs from S_1 at the bottom to S_7 at the top; **C**) and **D**) Relative amounts of different chain length polysulfide species derivatized with increasing concentrations (0.5–98 mM) of **C**) NEM or **D**) IAM. **E**) and **F**) Difference in polysulfide speciation using different preparation methods of Na_2S_4 with NEM (**E**) and IAM (**F**).

Conditions: **A**-**D**) Polysulfide solutions were made by dissolving 10 mM Na_2S_3 in ultra-pure water at 20 ^{o}C. Alkylating agent (NEM or IAM) concentrations were 0.5 mM, 1.0 mM, 2.0 mM, 4.9 mM, 9.8 mM, 9.8 mM, 39.2 mM and 98 mM, respectively. Alkylating agents were added 5 min after dissolving the inorganic polysulfide salt. Data was recorded after 10 min incubation with the alkylating agents and are representative of n = 5 experiments with similar results. **E** and **F**) Condition 1: Na_2S_3 dissolved directly in NEM or IAM containing buffer. Condition 2: Na_2S_3 dissolved in ultra-pure water then diluted in NEM or IAM containing buffer. Condition 3: Na_2S_3 dissolved in ultra-pure water then diluted in buffer then diluted in NEM or IAM containing buffer. For specific details see Supplementary Information.

Figure 4

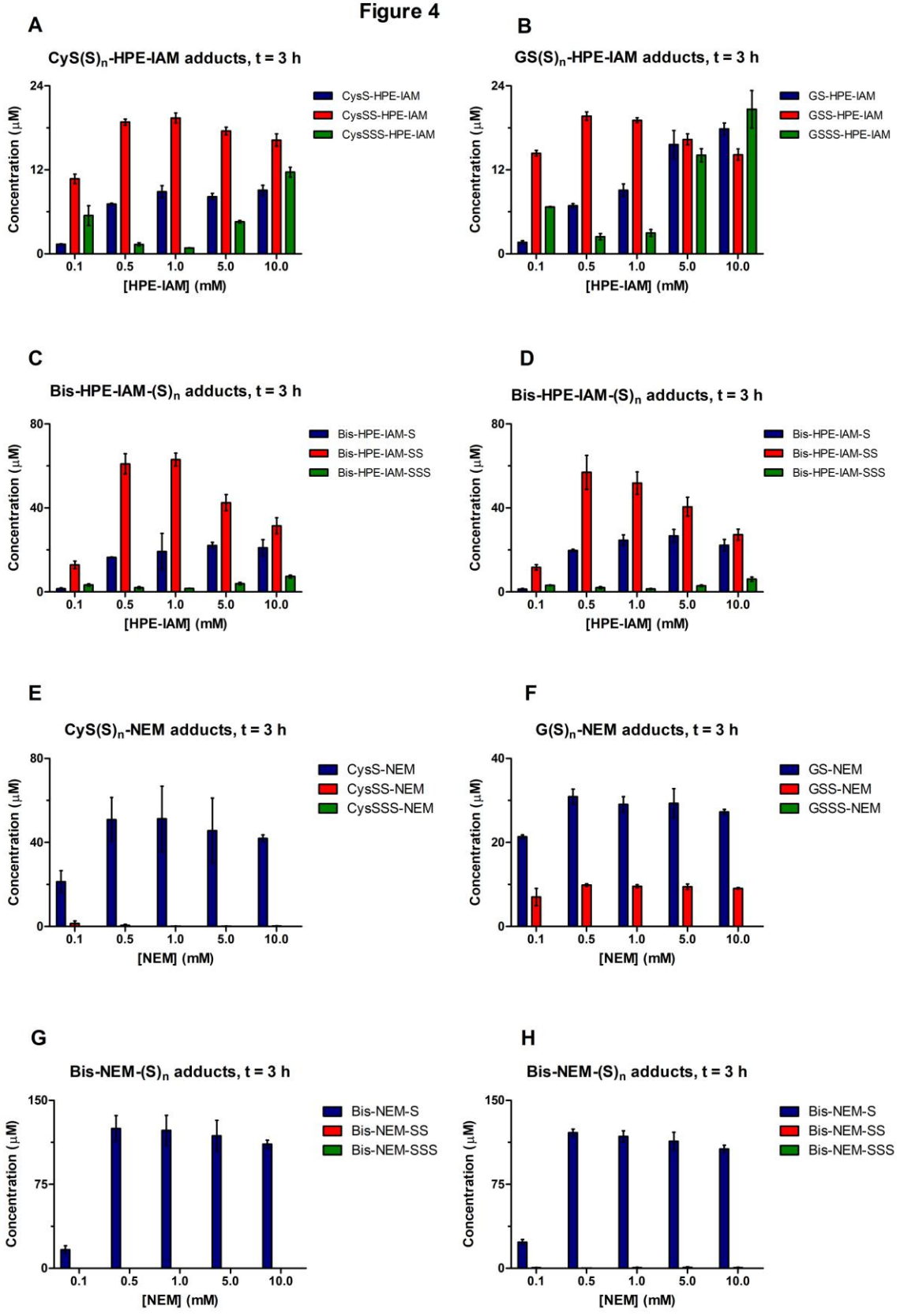

Figure 4: Quantitative measurement of derivatized Cys, GSH and inorganic polysulfide species, where derivatization was by 0.1–10 mM HPE–IAM (A-D) or by 0.1–10 mM NEM (E-H) A-B) Thiol, persulfide and trisulfide adducts of **A)** cysteine or **B)** GSH, treated with Na_2S_2, and then incubated with HPE-IAM for 3 hours. **C)** and **D)** represent the corresponding dialkyl sulfide or inorganic polysulfide adducts in the solutions of **A)** and **B)**, respectively. HPE-IAM had little effect on the speciation of the alkylated Cys and GSH persulfide species, but the detected alkylated trisulfide concentrations increased with the added HPE-IAM concentration.

E-F) Thiol, persulfide and trisulfide adducts of **E)** Cys or **F)** GSH, treated with Na_2S_2, and then incubated with NEM for 3 hours. Larger concentrations of NEM-captured-GSH-persulfides were observed than Cys-persulfides, with only a negligible effect of the concentration of NEM. **G)** and **H)** represent the corresponding dialkyl sulfide or inorganic polysulfide adducts in solutions of **E)** and **F)**, respectively.

Quantitation of sulfur species was achieved by using isotopically labelled internal standards as detailed in Materials and Methods. Data points represent the average of n = 3 independent experiments with the corresponding error bars showing the standard deviation. (Three different samples were prepared on three independent days for each condition.)

Conditions: 100 μM cysteine/GSH was treated with 300 μM Na_2S_2, at room temperature for 5 minutes, then incubated with 0.1–10 mM HPE–IAM or NEM at room temperature for 3 hours. Samples were prepared in 30 mM HEPES/KOH buffer (pH=7.5).

Figure 5

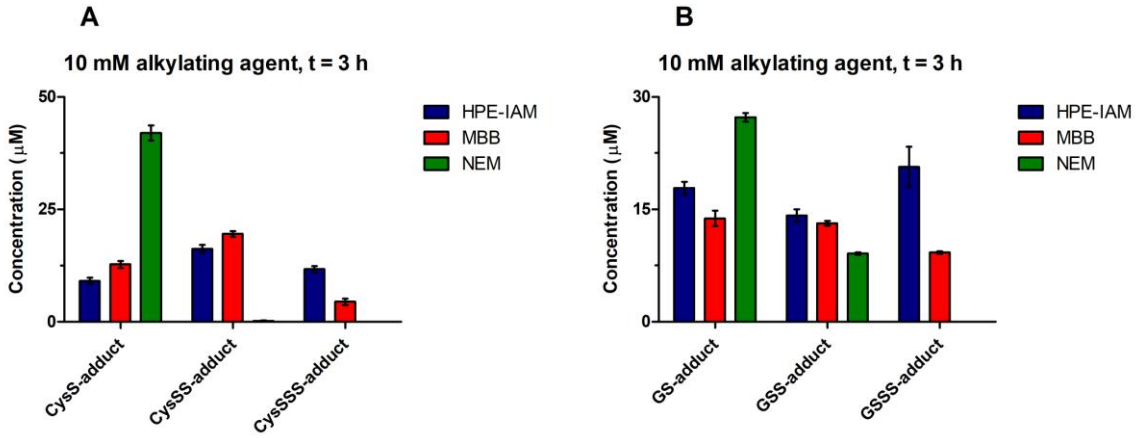

Figure 5: Relative measured quantities of derivatized Cys and GSH and their per- and trisulfide analogues using different alkylating agents. A) HPE-IAM and MBB alkylated cysteine per- and trisulfides were readily detected, while NEM is likely to cleave polysulfurchains and form thiol adducts instead **B)** The same phenomenon was observed in the case of the respective glutathione species, except NEM showing increased affinity and less –S-S- bond cleaving potential for glutathione-persulfide compared to Cys-persulfide.

Quantitation of sulfur species were achieved by using isotopically labelled internal standards as detailed in Materials and Methods. Data points represent the average of n = 3 independent experiments with the corresponding error bars showing the standard deviation. (Three different samples were prepared on three independent days for each condition.)

Conditions: 100 μM Cys/GSH was treated with 300 μM Na_2S_2, at room temperature for 5 minutes, then incubated with 10 mM alkylating agent at room temperature for 3 hours. Samples were prepared in 30 mM HEPES/KOH buffer (pH=7.5).

Figure 6

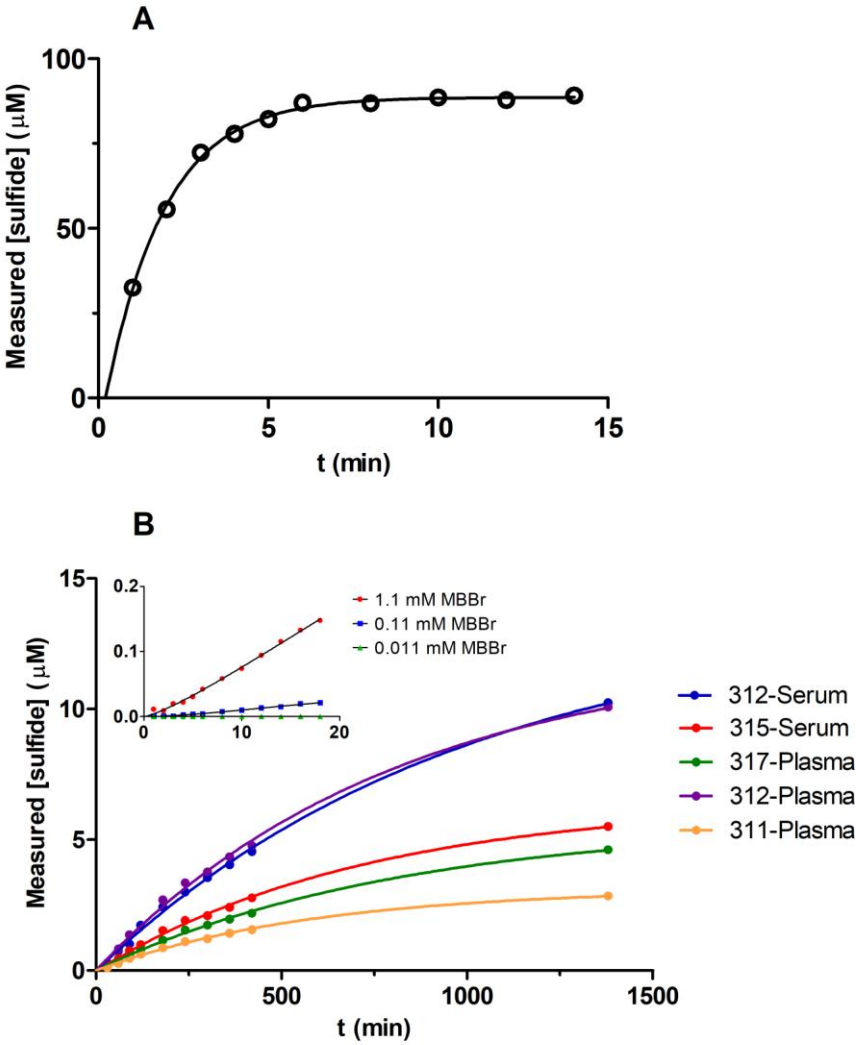

Figure 6: MBB-induced changes in sulfur speciation can confine sulfide detection in blood serum or plasma samples. A) Representative kinetic trace for the measured sulfide levels using the monobromobimane method in a 100 µM sulfide solution. Reaction was carried out at pH 8.2 with a final concentration of 1.1 mM MBB at room temperature. Measured data points fit perfectly to a first-order kinetic equation (black line) and it is clearly seen that the reaction completes in less than 10 minutes. **B)** Kinetics of sulfide-dibimane formation in blood serum or plasma samples during sulfide measurement with the monobromobimane method. Five different plasma or serum samples were derivatized under similar conditions as the sulfide standard solution on Figure 6A. The constantly increasing amounts of detected sulfide compared to Figurs 6A suggest that the observed kinetic curves

represent the extraction of sulfide from the biological sulfide pool (Nagy *et al.*, 2014) instead of direct alkylation of free sulfide. Moreover, the MBB concentration dependence of sulfide-dibimane formation in a representative blood serum sample (inset in Fig 6B) indicates that the detected sulfide levels using the monobromobimane method do not only depend on the incubation time, but also on the concentration of the alkylating agent. Conditions are detailed in the Methods section.

Figure 7

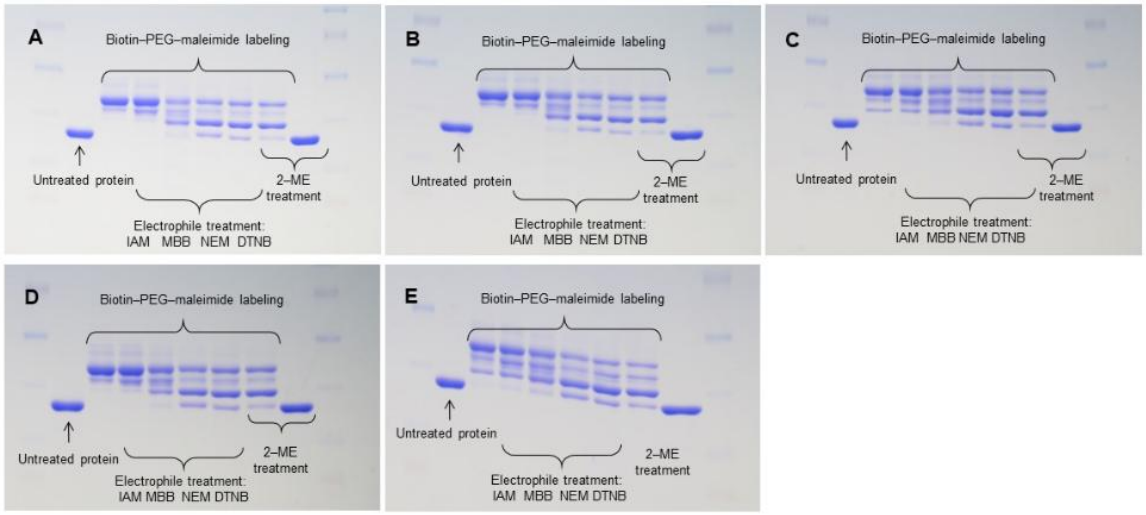

Figure 7: PMSA performed on human recombinant GAPDH showing the abilities of different chemicals to cleave alkylated protein polysulfide chains. All SDS-PAGE gels developed to detect GAPDH polysulfide species that were generated under different conditions showed similar pattern, indicating that the initial polysulfide treatment had no impact on the observed polysulfide speciation. NEM was most efficient among the applied alkylating agents to cleave the already alkylated Cys-polysulfide residues on the protein, MBB came next, and IAM had no cleaving effect. The fact that NEM and 2-mercaptoethanol or DTNB treatments showed a similar pattern suggests that NEM cleaved all Cys-polysulfide chains, corroborating our previous observations. Human recombinant GAPDH **A**) control sample with no polysulfide treatment or treated with **B**) 0.1 mM Na_2S_2, **C**) 1 mM Na_2S_2, **D**) 0.1 mM Na_2S_3 or **E**) 1 mM Na_2S_3 then labeled with biotin-PEG-maleimide, followed by incubation of various electrophile agents (IAM, MBB, NEM and DTNB respectively) or 2-mercaptoethanol.

Conditions: 1 h incubation with 0.1 mM or 1 mM Na_2S_2/Na_2S_3 at 37 °C followed by 1 h incubation with 2 mM biotin-PEG-mal at 37 °C, then 1 h incubation with 3 mM alkylation agent (IAM, MBB, NEM, DTNB) at 37 °C. Samples were heated in the presence or absence of 5% 2-mercaptoethanol, then separated by SDS-PAGE and stained using CBB. Samples were prepared in 10 mM RIPA buffer (pH=7.4).

Figure 8

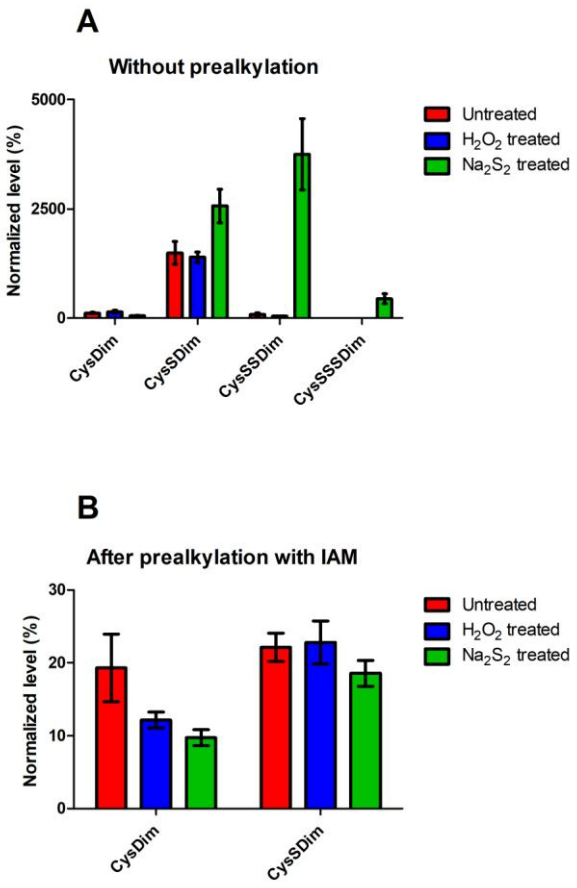

Figure 8: Normalized levels of Cysteine-dimedone (CysDim) and Cysteine–per/polysulfide-dimedone (Cys-S_xDim x = 1-3) adducts in digested GAPDH samples after treatment with hydrogen–peroxide or inorganic polysulfides with or without prealkylation with IAM. A) More dimedone labelled Cys polysulfide derivatives were detected when the isolated protein was treated with inorganic polysulfides compared to H_2O_2-treated or untreated samples. Remarkably, significant amounts of Cystein-persulfide dimedone adducts were measured, despite of prereduction, which could be attributed to GAPDH Cys residues that are not exposed to the solution (and hence not reduced during the prealkylation step, see Figure 7). Data points represent the average of n = 5 independent experiments with the corresponding error bars showing the standard error of mean. (Three different samples were prepared on three independent days from each condition.) **B)** Decrease by orders of magnitude in all dimedon adducts was observed in prealkylated samples, which suggests that alkylation with IAM can effectively hinder sulfenic acid

formation/detection. Data points represent the average of n = 5 independent experiments with the corresponding error bars showing the standard error of mean.

All peak areas were normalized to the average areas of the Cys-dimedone in untreated samples without prealkylation (Fig 6A, CysDim). Conditions are detailed in the Methods section.

Figure 9

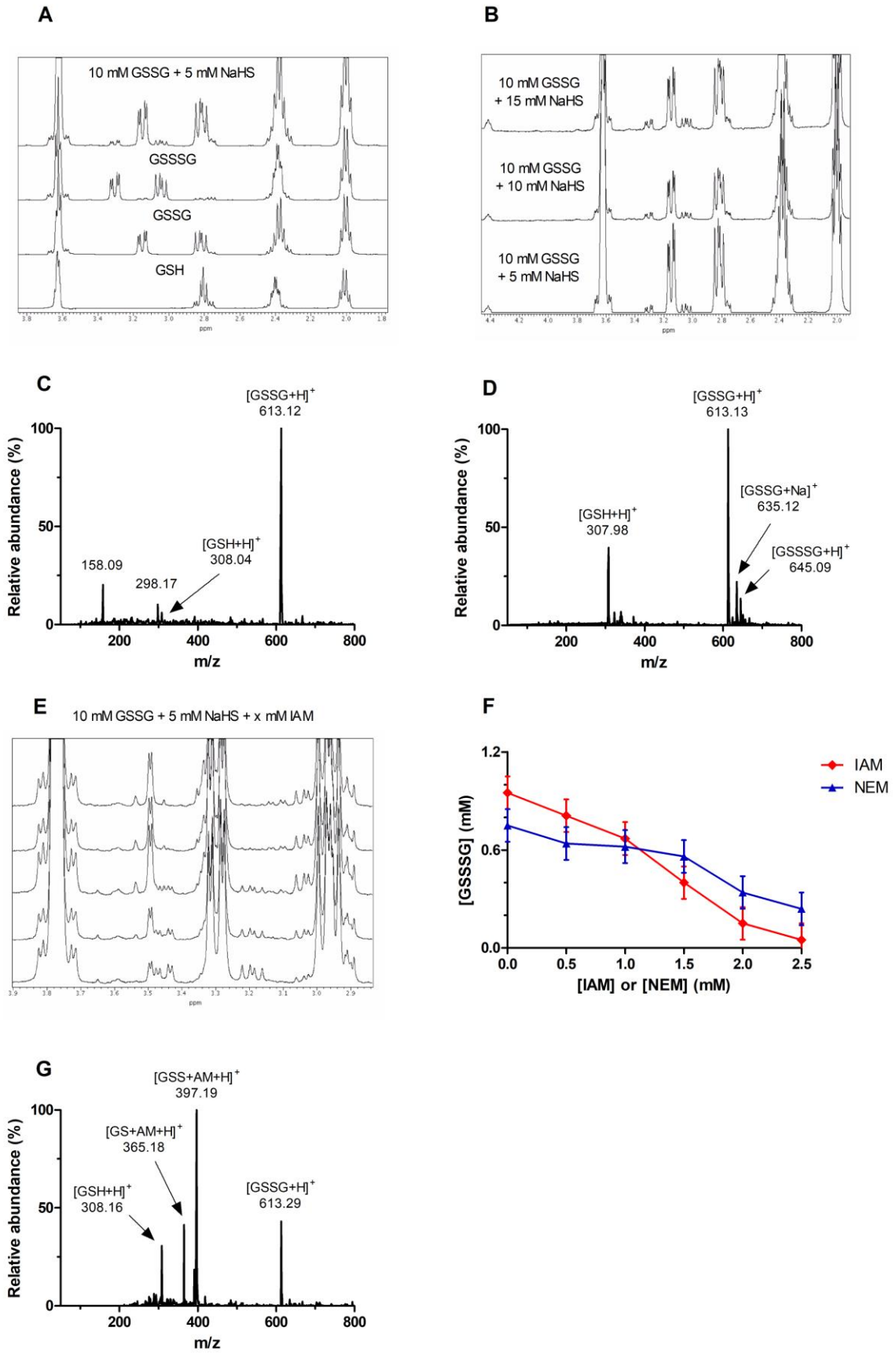

Figure 9: ^{1}H-NMR and direct infusion mass spectrometry measurements for detecting GSH-polysulfide speciation in the absence or in the presence of IAM or NEM **A**) Selected region for the stacked ^{1}H-NMR spectra of GSH, GSSG, GSSSG and GSSG + NaSH, as indicated. The new peaks formed after equilibration of GSSG with NaSH correspond to GSSSG (δ = 3.16-3.22 and 3.43-3.48 ppm), as indicated by comparison with standard GSSSG. **B**) Selected region for the stacked ^{1}H-NMR spectra of GSSG samples incubated with increasing additions of NaSH. Increasing addition of NaSH caused subsequent increases in the amount of GSSSG (δ = 3.16-3.22 and 3.43-3.48 ppm) and GSH (δ = 4.56 ppm) produced. **C**) ESI-MS spectra of GSSG **D**) ESI-MS spectra of GSSG equilibrated with NaSH. Identified species are indicated in each spectrum. **E**) Selected region for ^{1}H-NMR spectra of GSSG + NaSH with increasing additions of IAM (bottom to top spectrum, respectively). Increasing addition of IAM causes subsequent decreases in the concentration of GSSSG (δ = 3.16-3.22 and 3.43-3.48 ppm), likely because IAM is competitive with GSSG for the trapping of the intermediate GSSH. **F**) Concentration of GSSSG in equilibrated samples of GSSG and NaSH as a result of increasing exogenous addition of the electrophiles IAM (black squares) and NEM (black diamonds). Data points represent the average of n = 3 independent experiments with the corresponding error bars showing the standard error of mean. **G)** ESI-MS spectrum resulting from the addition of IAM to an equilibrated solution of GSSG + NaSH. Addition of IAM reacts, and traps GSH ($[GS+AM+H]^{+}$) and GSH persulfide (GSSH, $[GSS+AM+H]^{+}$).

Conditions: For ^{1}H-NMR measurements, 10 mM GSSG was incubated with 5–15 mM NaSH at room temperature for 30 minutes, followed by incubation with 1–5 mM IAM at room temperature for 1 hour for derivatization measurements. Spectra were measured in 100 mM phosphate buffer (pH 7.4) with 10 % D_2O and 1 mM DSS as an internal reference. For ESI-MS measurements, 1 mM GSSG was incubated with 0.5 mM NaSH at room temperature for 30 minutes, followed by the addition of 0.5 mM IAM and incubation at room temperature for 1 hour for derivatization measurements. Spectra were measured in 50 mM ammonium bicarbonate buffer (pH 7.4).

Figure 10

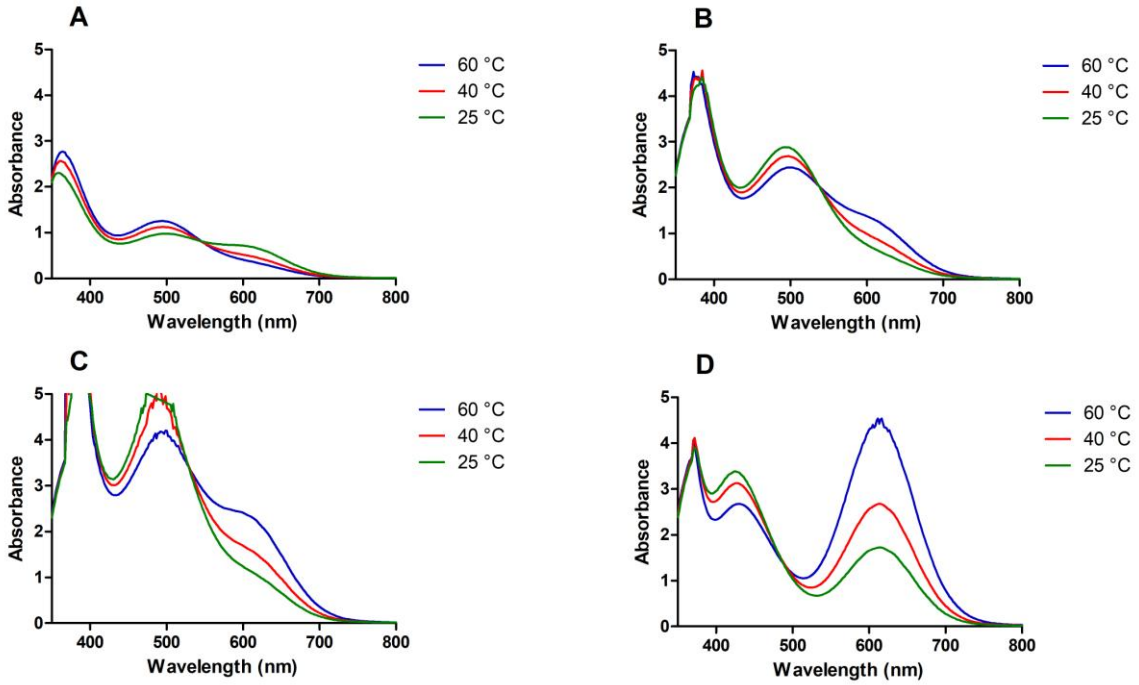

Figure 10. UV-Vis spectra of organic polysulfides as a function of temperature in organic media. A) UV-Vis spectra show changes in speciation of organic polysulfides as a function of temperature in organic media in a mixture with molar ratios of S_8 over NBu_4SH of **A)** 1:1, **B**) 1:2, **C**) 1:3, and **D**) 1:8.

Conditions: 10 mM S_8 in dry, air-free deuterized tetrahydrofuran; 10-80 mM NBu_4SH dry, air-free deuterized acetonitrile, T=25, 40 and 60 °C.

Table 1. Theoretical and observed masses for polysulfide radical ions, thiosulfate and other observed species in the experiment depicted on Figure 1 D-F.

	Exact Mass (amu)	Measured Mass (amu)	Difference (amu)	Difference (ppm)
$S_2^{\cdot-}$	63.9448	63.9469	0.0021	33
$S_3^{\cdot-}$	95.9168	95.917	0.0002	2
$S_4^{\cdot-}$	127.889	127.9057	0.0167	131
$S_2O_3^{\cdot-}$	111.9294	111.9312	0.0018	16
$HS_2O_3^-$	112.9367	112.9398	0.0031	27
HSO_4^-	96.9596	96.9599	0.0003	3

Table 2. Relative percentages of trapped benzyl polysulfides. All quenches were performed at room temperature unless noted otherwise.

		1:1	1:2	1:2 (40 °C)	1:2 (60 °C)	1:3	1:4	1:8
Bn_2S_2	(3.74 ppm)	0	0	0	0	0	0	2.4
Bn_2S_3	(4.11 ppm)	41	42.5	42.6	41.9	47.3	37.2	87.2
Bn_2S_4	(4.24 ppm)	32.5	32.2	32.3	32.4	32.2	25.4	10.3
Bn_2S_5	(4.29 ppm)	26.5	25.3	25.1	25.7	20.5	37.4	0